Thin-Walled Structures 180 (2022) 109953

Contents lists available at ScienceDirect

Thin-Walled Structures

journal homepage: www.elsevier.com/locate/tws

Full length article

A critical review of cold-formed steel seismic resistant systems: Recent developments, challenges and future directions

Maryam Hasanali [a,*,1], Krishanu Roy [b], Seyed Mohammad Mojtabaei [c], Iman Hajirasouliha [c], G. Charles Clifton [a], James B.P. Lim [a,b]

[a] Department of Civil and Environmental Engineering, The University of Auckland, New Zealand
[b] School of Engineering, The University of Waikato, Hamilton 3216, New Zealand
[c] Department of Civil and Structural Engineering, The University of Sheffield, Sheffield, UK

ARTICLE INFO

Keywords:
Cold-formed steel (CFS)
Lateral force-resisting systems (LFRS)
Braced-wall systems
Moment-resisting frames

ABSTRACT

Cold-formed steel (CFS) systems have seen an increased application in the past few decades, especially in the construction of low- to mid-rise buildings. CFS members offer considerable structural and environmental advantages, such as low weight, ease and speed of construction, greater manufacturing flexibility, recyclability and low embodied carbon. Despite the significant potential offered by CFS structural systems, the seismic design of lateral force-resisting systems (LFRS) for CFS multi-story buildings is challenging. There are many different types of systems capable of providing the lateral load resistance capacity of the CFS framing, and this paper provides a comprehensive review of the research developments made in CFS braced-wall systems and moment-resisting frames, as the most conventional systems, to study their structural performance and identify the research gaps, challenges, and future directions. The major research developments are summarised in terms of load capacity, stiffness, energy dissipation capacity and failure mode. As an outcome of the crucial review, it was found that CFS LFRSs can generally offer more efficient design solutions regarding seismic characteristics such as high ductility and energy dissipation capacity. Despite a rather large body of research on CFS braced walls, it is necessary to assess the response of these systems in various aspects, such as developing an optimisation framework to withstand the combination of vertical and horizontal loading plus resist the impact of severe fire. With respect to moment-resisting frames, one of the main research needs is to develop systems suitable for multi-story buildings, especially in seismic regions.

1. Introduction

In recent years, cold-formed steel (CFS) elements have been increasingly used as primary structural elements in low- to mid-rise buildings [1,2] and in portal frames with short to intermediate spans [3]. Gad et al. [4] classified the factors influencing the behaviour of CFS structural systems under lateral loading, into six categories: (i) frame properties (i.e., material properties of the frame and hold-down system, aspect ratio, and stud spacing); (ii) cladding (material, thickness and orientation, number of cladded sides, type and configuration of fasteners); (iii) bracings (material, type of bracing and member properties, fixity details, and initial tension level); (iv) cladding and bracing interactions; (v) boundary conditions (set corner joints, ceiling cornices, skirting boards, and vertical loads); and (vi) size and location of openings.

One of the remaining challenging issues is to develop lateral force-resisting systems (LFRS) suitable for mid- to high-rise constructions, especially in high seismic regions. Compared to traditional hot-rolled steel braced and moment frame systems, the thinness of CFS members makes it difficult to provide sufficient rigidity at the connections [5], and therefore, most of typical CFS elements are only partially restrained. As a result, CFS moment frame systems are generally considered inefficient under seismic loads [6]. In CFS framing, close spacing of members has been proven to be the most efficient arrangement for gravity loading. However, this complicates concentric bracing through the webs since multiple members need to penetrate over a single diagonal brace [7]. As a result, lateral systems for CFS framing follow more of the traditions used in timber construction, which can be a challenge for the engineer well-versed in hot-rolled steel systems.

A bare standard CFS frame including only studs and tracks (Fig. 1(a)) has just 5% of the total frame strength [5], so it is insufficient to withstand lateral loads. LFRSs for CFS structures fall into one of the following categories: (i) various types of board sheathings; (ii) diagonal strap-braced walls; (iii) K-braced walls; (iv) moment-resistant

* Corresponding author.
E-mail address: mhas455@aucklanduni.ac.nz (M. Hasanali).
[1] PhD candidate

https://doi.org/10.1016/j.tws.2022.109953
Received 29 April 2022; Received in revised form 6 July 2022; Accepted 1 August 2022
Available online 12 September 2022
0263-8231/

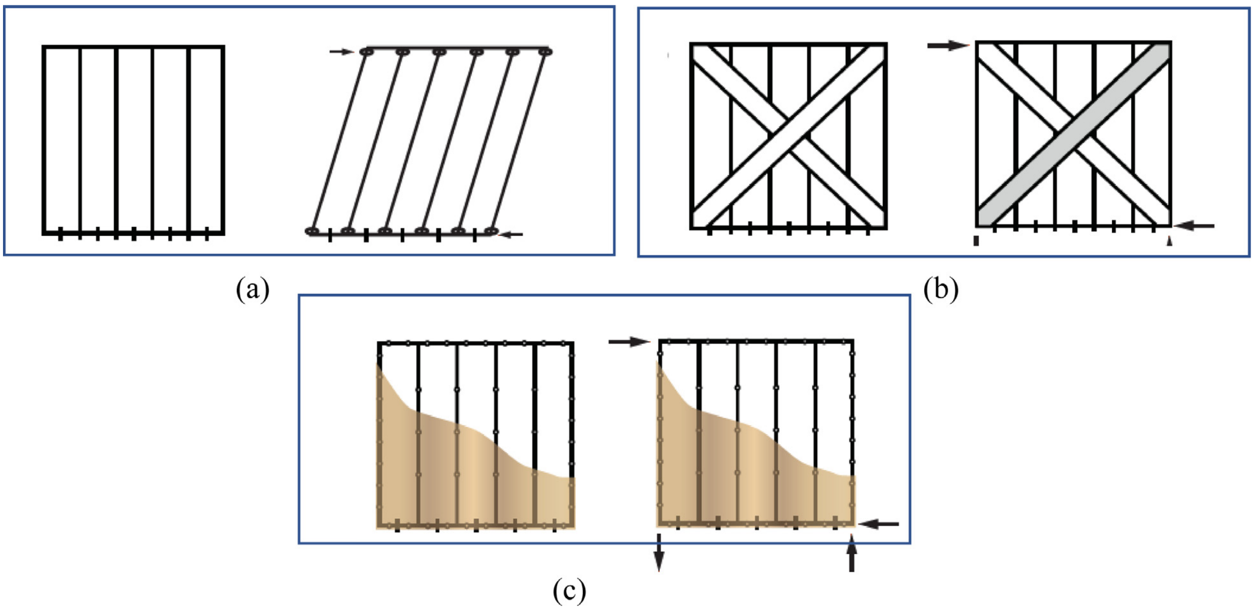

Fig. 1. Cold-formed steel framed panels (a) bare panel with little to no lateral resistance (b) strap-braced panel (c) sheathed panel [5].

frames; (v) podium-type structures, in which a complete load bearing CFS frame is built atop of other structures; and (vi) hybrid systems, in which reinforced concrete or hot-rolled steel elements are used to resist the lateral loads. Among the listed categories, strap-braced walls (Fig. 1(b)) and sheathed panels (Fig. 1(c)) are the two most prevalent forms. While in the design of CFS braced shear walls, the behaviour of the wall is determined by the brace tension strap size and steel grade, for CFS sheathed shear walls, the sheathing type and fastener pattern are the key factors to meet the required strengths. The CFS frames can be sheathed with different materials such as wood-based boards, flat steel sheets [8] and corrugated steel sheathing [9–12].

Two different methods have been introduced to design CFS members against seismic actions: the "sheathing-braced" and the "all-steel" approach [13]. In the case of the "sheathing-braced" approach, the high stiffness of the sheathing contributes to the axial and flexural capacity of the steel elements by increasing their resistance to global, local, and distortional buckling. Furthermore, this material participates in resisting in-plane lateral forces through its diaphragm stiffness. However, current design standards such as AS/NZS 4600 (2018) [14] do not fully take into account the design provisions for composite action between the studs and the sheathing; instead, they contain an "all-steel" design approach [13] unless the performance of the system is determined by test. In this case, the stiffness, strength, and lateral restraint provided by the sheathing panels do not play a significant role in the lateral resistance of the CFS frame, and the structure is composed of steel elements, in which bracing members are necessary to resist lateral forces [15]. With respect to the shear walls with steel sheet sheathing, an analytical design model called the "Effective Strip Method" was developed by Yanagi and Yu [16] and prescribed by AISI S210 [17] and S400 [18]. According to this method, a sheathing strip carries the lateral load via a tension field action, while the tensile strength of the shear wall is controlled by the tensile strength of the effective sheathing strength.

Although the majority of the previous studies have focused on the behaviour of shear wall panels as the main lateral force-resisting system, using CFS moment-resisting frames provides greater flexibility for space planning by reducing the reliance on fixed shear wall panels. Furthermore, CFS moment-resisting frames can improve the energy dissipation capacity and seismic performance of CFS structures under strong earthquakes [19]. Currently CFS moment-resisting systems are mainly limited to one-story framing systems used in industrial construction. Friction and bearing at the bolted connections of CFS frames are key factors that help them to withstand inelastic deformations by providing a ductile yielding mechanism [5]. The strong column–weak beam design philosophy associated with structural steel moment frames is not appropriate for this system, however, strong column-weak connection design philosophy can be used. CFS moment-resisting systems have semi-rigid connections which rely on inelastic action through slippage and bearing in the bolted beam-to-column moment connections to form a ductile yielding mechanism. Beams and columns should remain elastic using capacity design principles [20].

Over the past two decades, extensive experimental and numerical research has been carried out to study the behaviour of CFS braced stud wall systems and moment-resisting systems. This paper aims to bring together recent research developments on these systems in order to gain a better understanding about their structural performance and identify research gaps and challenges for their further development. To this end, the available research studies were summarised in two main sections, namely braced shear walls and moment-resisting systems. These sections were then classified further based on the research methodologies employed in the reviewed papers, while the major research developments and challenges were critically reviewed. The effects of key design parameters on the structural performance of CFS braced shear walls and moment-resisting frames were classified and summarised in terms of load capacity, stiffness, ductility, energy dissipation capacity, and the failure mechanism at the end of each section. The research methodologies used in the existing literature, the loading protocols, connection types, and failure mechanisms, as well as the research highlights for improving the lateral performance of these systems, were classified in the tables reported in Appendices A to C. Finally, recommendations were provided to map future research directions to achieve more efficient and sustainable CFS LFRSs.

2. Braced shear walls

CFS braced shear walls generally consist of a steel frame comprised of top and bottom tracks made with unlipped channel sections (U-shaped), intermediate studs, and chord studs having lipped channel sections (C-shaped), and various configurations of braces [21]. To reduce the buckling length of the vertical elements, a nogging element is also used at the wall's mid-height (see Fig. 2). In this type of LFRS, the lateral load is basically resisted through truss (axial) action by employing braces on one or both faces of the wall panels [22]. The

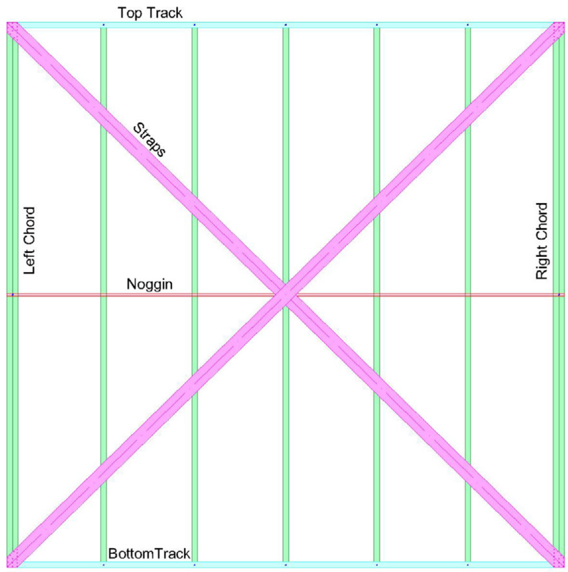

Fig. 2. Configuration of a CFS strap-braced wall.

lateral loads are carried from the braces to the chord studs and through the hold-down devices to the anchor rods, eventually finding their way into the foundation [15]. In this process, an appropriate load path for transferring the brace load to the supports is crucial to avoid stud-to-track connection failure. The braces are considered active only in tension because of their high slenderness, leading to low buckling capacity [23,24]. In a study by Velchev et al. [25], the reinforcement of the terminal fields of the track was recommended to avoid the local buckling arising from the compression transmitted by diagonal members. This indicates that the design of members and connections located at wall corners is crucial [21], as is the wall/floor/wall connection between adjacent stacked strap-braced wall panels.

The main research developments of different types of braced shear walls based on the research methodologies (i.e., experimental, numerical, and analytical) are summarised as follows.

2.1. Strap-braced walls

Over the past two decades, the behaviour of CFS strap-braced stud wall systems under monotonic, cyclic, and seismic loading has been widely investigated. The objectives of most research studies have been to investigate the wall behaviour in terms of lateral load capacity, stiffness, ductility, energy dissipation capacity, and failure modes. The effects of the following aspects have been examined on the structural performance of the walls: (i) strap bracing behaviour (i.e., bracing side, strap dimensions, and steel material properties); (ii) type of the connections of frame-to-strap (i.e., screws, bolts, and welds); (iii) wall corner details; (iv) wall aspect ratio; and (v) loading type. A summary of experimental, numerical, and analytical research on CFS strap-braced walls is provided in Tables A.1, A.2, and A.3 in Appendix A, respectively.

2.1.1. Experimental investigation

The effect of the strap bracing behaviour on the lateral performance of the wall specimens has been investigated by taking into account the influence of various strap dimensions, steel material properties, and strap braces on one or both wall sides. The geometry of straps in terms of the strap width and thickness has been evaluated by [26–28]. They concluded that the use of wider straps increased the lateral resistance and stiffness, as well as providing more room for connections. Furthermore, it was shown that varying the strap's width significantly affects the deflection of a frame, however, it has little influence on its racking load capacity. On the other hand, a frame without bracing has very low racking resistance [26]. In addition, the use of thicker straps [29] has shown to provide a higher capacity as greater thickness increases the connection capacity in bearing, tilting and pull-out according to AS/NZS 4600 [14], provided non-ductile modes of failure are suppressed. The effective length of the X-bracing systems can be used to determine their compression strength and characterise their hysteretic response, including their energy dissipation capacity [30]. If the strap braces are replaced with hollow section bracing members, with much higher slenderness ratios, then the effective length of the X-bracing can be used to determine their compression strength and characterise their hysteretic response, including their energy dissipation capability [30]. Fig. 4 adopted from Kasaeian [31], compares the wall performance in terms of maximum shear and ductility using different strap thicknesses. It can be seen that increasing the strap thickness can generally increase the maximum lateral load capacity of the wall systems, while it may lead to lower ductility levels. However, the results of Kasaeian [31] study indicated that the lateral performance of the panel was not affected by the stud spacing and the change in the length of the fuse.

Concerning the material properties of the wall frame, it was proposed to use a bracing force greater than the minimum specified value of strap yield strength for the design of chord studs, tracks, and frame-to-strap connections [32], thus imparting a dependable yielding mechanism. Similarly, the study by Casafont et al. [33] showed that the ductile behaviour and dissipation capacity of the tested walls were increased by using lower steel grade for the straps than for the other members. Kasaeian et al. [31] also concluded that the straps with higher strength prevent the wall penal from reaching the full yielding capacity of the braces. Therefore, to achieve a ductile response, strengthening the brace must be compatible with the strength of the other elements and not force a sudden mode of failure into the chords or tracks.

With respect to the bracing side, Serrette and Ogunfunmi [28] demonstrated that the excessive lateral deflection led to a failure in one-sided X-braced walls. As expected, the maximum load capacity of one-sided X-braced walls was around 50% of that of the similar two-sided X-braced ones. The results of the study conducted by Tian et al. [26] confirmed the aforementioned finding. Adham et al. [27] also evaluated the in-plane lateral load–deflection characteristics of CFS stud walls with gypsum wallboard panels and diagonal strap braces under lateral cyclic load imposed by wind or earthquake. The results of this study highlighted that the compressive diagonal straps do not contribute to the lateral strength of the walls. In addition, the one-sided strap-braced walls were subjected to an eccentric loading, causing local buckling instability in tracks and chord studs as a result of the combined action of bending and axial load. In this case, a premature wall failure occurred before the development of the strap capacity [32].

The capacity-based design approach is used in most standards to design strap-braced walls. Based on this procedure, the diagonal tension braces are assumed to act as inelastic fuse elements in the pin-connected seismic force-resisting system, to ensure all other elements remain undamaged under loading. In the studies of Mirzaei et al. [23], Velchev et al. [25], and Comeau [34], the responses of walls with different aspect ratios have been compared. The results of these studies confirmed the accuracy of the capacity-based design assumption for walls with aspect ratios (i.e., height-to-length ratios) closer to 1. A more ductile behaviour was seen in the walls with aspect ratios of 1:1 and 2:1 rather than those with an aspect ratio of 4:1, in which the chord studs failed prematurely due to combined axial compression and bending moment with a significant reduction in the lateral stiffness. It was also revealed that a significant moment might be generated in the chord studs at the strap connection location in the strap-braced walls with aspect ratios of over 1.9:1. Fig. 3(a) to (d) show the compression and flexural failure of chord stud for walls with 2:1 and 4:1 aspect ratios as well as yielding and net cross-section fracture of braced-wall for walls

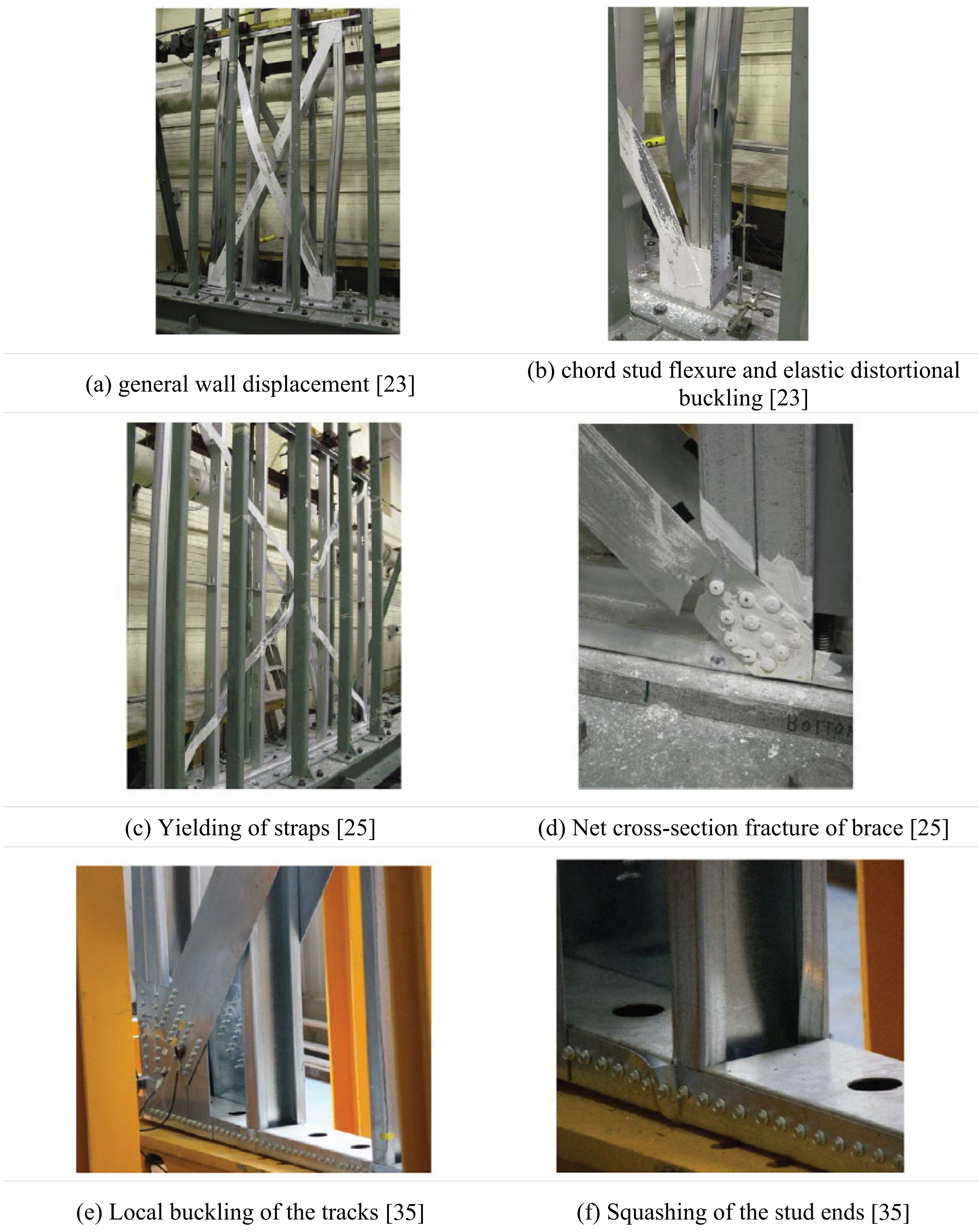

(a) general wall displacement [23]
(b) chord stud flexure and elastic distortional buckling [23]
(c) Yielding of straps [25]
(d) Net cross-section fracture of brace [25]
(e) Local buckling of the tracks [35]
(f) Squashing of the stud ends [35]

Fig. 3. Different failure modes of strap-braced walls.

with an aspect ratio close to 1. The results of the study by Fiorino et al. [35] confirmed the requirement for using a capacity-based design method in the design of strap-braced walls due to the brittle failure modes of walls designed without a capacity-based design approach.

Velchev and Rogers [36] also pointed out that a capacity-based design approach should be used to achieve high ductility and energy dissipation. They concluded that the connection design rules specified by AISI S213 (2012) [37] effectively prevent non-ductile modes of failure and improve the lateral performance of the stud walls. Strap-braced walls with welded connections were the subject of a study by Comeau [34] and Velchev et al. [25]. The results of their study also showed a ductile behaviour. It was also recommended to avoid the use of strap-braced walls having aspect ratios greater than 2:1 unless the moments associated with flexure of the chord studs are included in the capacity design procedure for the studs. Kasaeian et al. [31] developed a new CFS strap-braced wall panel in compliance with the

(g) Out-of-plane deformation of gusset plate [35]

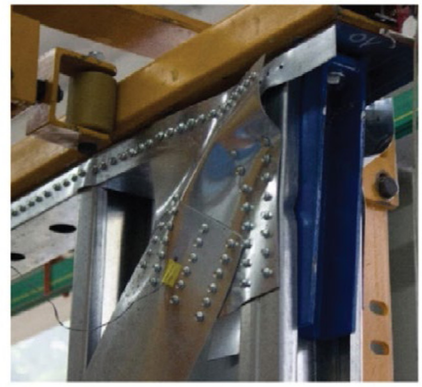

(h) Gusset-to-track connection failure [35]

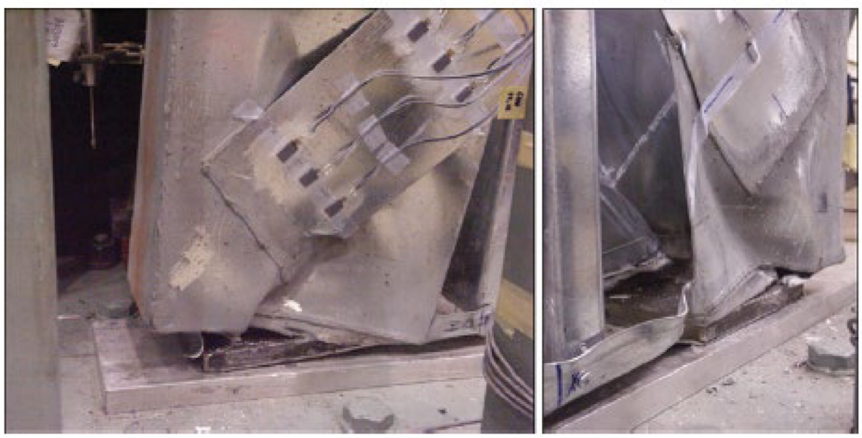

(i) Punching shear failure mode at hold-down location [38]

(j) Bearing failure [29]

(k) Bearing and tilting failure [29]

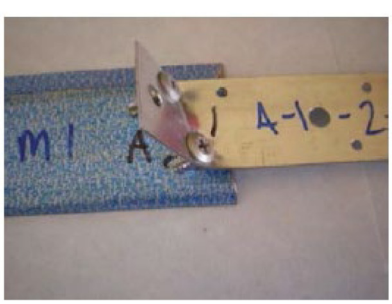

(l) Tilting failure [29]

(m) Pull-out failure [29]

Fig. 3. (*continued*).

capacity-based design principles, allowing energy dissipation of braces through the yielding of a fuse element. Six different configurations of strap-braced walls (see Table 1) were evaluated through experimental, analytical, and numerical procedures. The results indicated that the

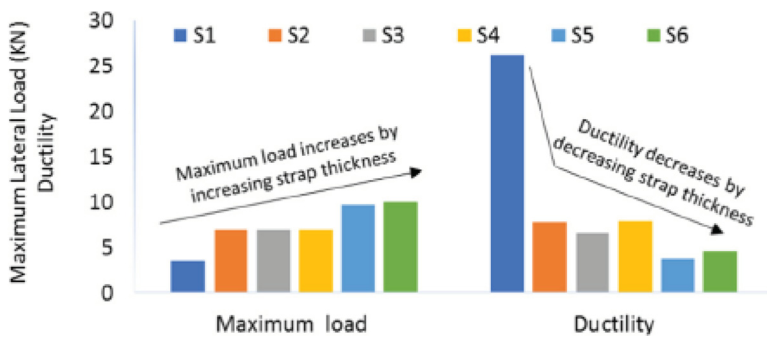

Fig. 4. Comparison of wall performance in terms of maximum shear and ductility [31].

Table 1
Specimen configuration.

Specimen	Stud spacing (mm)	L_{fuse} (m)	Thickness (mm)	Yield stress (MPa)	Ultimate stress (MPa)	Bracing side
S1	600	1.5	0.6	290	348	One side
S2	400	1.5	0.6	290	348	Both sides
S3	600	1	0.6	290	348	Both sides
S4	400	1	0.6	290	348	Both sides
S5	400	1	1	315	382	Both sides
S6	600	1.5	1.25	370	436	Both sides

failure mode of specimens $S1$ and $S2$ was strap yield with large elongation in the fuse, however, the prevailing failure of $S3$ and $S4$ appeared in the tension straps followed by the localised partial distortion in the top track of specimen $S3$. In specimen $S5$, the brace-to-frame screws' pull out caused some distortional buckling with flange rupture in the lower track, while the left corner of the top track underwent local buckling, and some distortional buckling was observed in this area after the screw tilting.

In general, an individual member's failure is more desirable than a failure in a connection in which several members may be affected. The CFS strap-braced walls' connections fall into three configurations: (i) the straps connect directly to the chords through self-drilling screws [38]; (ii) the gusset plates are utilised to connect the straps and chords via self-drilling screws [21]; and (iii) the straps connect through welding to gusset plates [38] (see Fig. 5). The connections between the strap-braced walls are mostly self-drilling screws, which are sometimes accompanied by gusset plates [21,25,35,36,38,40–42]. Since the gusset plates bring an enhancement in capacity, they are preferred when greater forces are applied to the structure. The gusset plates cause an increase in the number of screws, and in turn, the buckling of the bottom track would be avoided due to the more even distribution of forces [36]. The performance of welded strap-braced walls has been also investigated by [23,25,34]. In general, these studies indicated more ductile behaviour in walls with aspect ratios of 1:1 and 2:1 as opposed to those with a 4:1 aspect ratio.

Casafont et al. [33] conducted tests on main connection systems to investigate the local behaviour of CFS walls. Different failure modes were observed in the tests, including bearing, tilting, pull-out, pull-through, net section failure, shear failure of the connection device, punching, tearing, and local buckling. Net section failure is the preferred mode for seismic design because it provides enough strength to allow the cyclic yielding of the diagonals, and it leads to the most ductile connection behaviour. In a similar study, Fiorino et al. [35] observed four failure modes during both monotonic and cyclic tests: (i) local buckling of the tracks at the elastic part of the response curve (Fig. 3(e)); (ii) squashing of the stud ends (Fig. 3(f)); (iii) out-of-plane deformation of the gusset plate connected to the diagonal tension strap (Fig. 3(g)); and (iv) gusset-to-track connection failure in correspondence of a significant reduction of strength on the response curve post-peak branch (Fig. 3(h)). They also showed that the inelastic performance of the wall can be adversely affected by non-ductile phenomena, such as the gusset-to-track connection failure and combined bending and compression axial load failure of the chord studs. In general, monotonic and cyclic tests showed that the stud wall systems might exhibit non-ductile seismic performance, due to gusset-to-track connection failure or compression buckling failure of the track.

The performance of tensile bolted and screwed joints of the strap-braced walls have been investigated in terms of their failure modes, force–displacement curve, ductility and stiffness by Casafont et al. [43,44]. It was demonstrated that the X-braced walls can provide high energy dissipation capacity via plastic deformation of diagonal straps, while they also increase the lateral stiffness of CFS structures. In general, it was shown that bolted connections are less adequate than screwed connections in terms of ductility and strength. In a follow-up study [33], they also recommended using screws rather than bolts for connection devices, in which the more net-section area is available due to their smaller diameter.

A large number of studies have been carried out to investigate the failure modes of strap-braced walls and to provide measures to avoid the undesirable failure modes. Moghimi and Ronagh [39] showed that the use of double-section chords strengthens the track-to-stud joints under bearing failure and provides more room for the insertion of screws that connect the strap to the wall panel. Strap bracing Type I (see Table 2) rendered unacceptable results, which was attributed to premature distortional buckling of the left and right studs at earlier stages of the racking displacement, causing most of the strap load to be transferred to the track and bending them significantly. Gad et al. [4] tested the lateral resistance and behaviour of unlined frames braced with straps, plasterboard lined walls, and plasterboard lined walls with strap braces. The results showed that the strap bracing system governed the behaviour of domestic unlined CFS systems, while the type of fixity of the strap bracing to the top and bottom plates and the presence of the tensioner unit affected the failure load and mechanism. The failure mechanism of unlined frames was governed by tearing the strap at the strap-to-frame connection or at the tension unit location. This brittle failure mode can be eliminated by using a carefully perforated strap, a solid strap with a sufficient ratio of ultimate to yielding stress, and brackets or gusset plates. They also demonstrated that the initial tension in the strap braces increases the frame stiffness and consequently affects the initial dynamic characteristics of the frame. Brace failure was reported in two modes: (i) net cross-section fracture, and (ii) connection failure (combination of bearing and pull-out or punching shear failure).

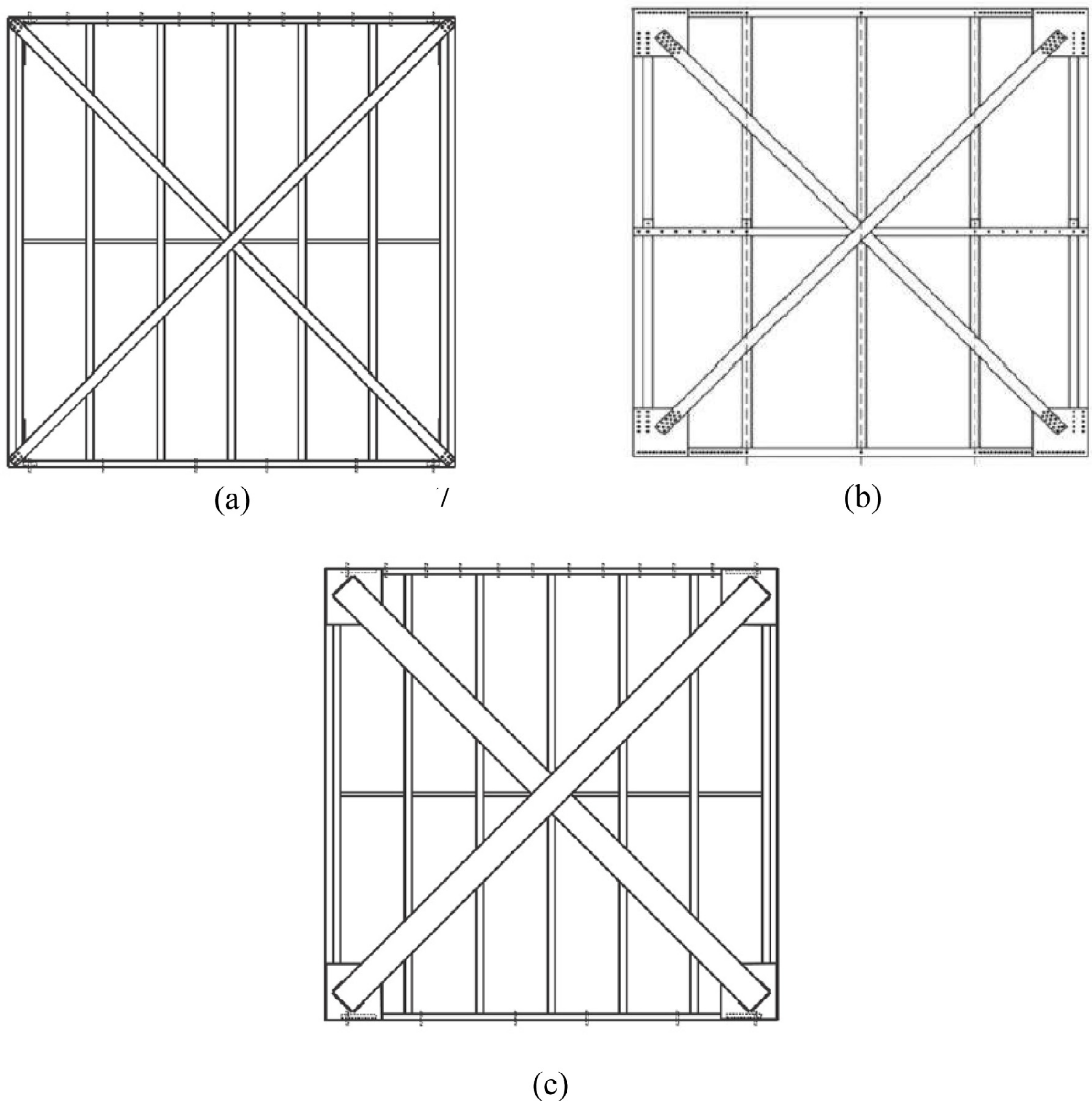

Fig. 5. Different types of strap-braced walls' connections: (a) simple screws [38] (b) all-screw connected through gusset plates [21] (c) all-welded with gusset plates [38].

According to [43,44], the tilting failure was prominent in the joint connecting two straps of the same thickness, whereas the bearing was evident in the joints connecting two straps of different thicknesses. It should be noted that, in general, yielding of the diagonal straps prior to joint failure is required for seismic design of X-braced shear walls with undefined section failure. There are different ways to create the net section failure, for instance, placing enough screw connections in the joint to avoid bearing, connecting two steel sheets of different thicknesses (i.e., a thin diagonal strap with a thick gusset) and the use of washers in bolted connections. These studies also compared the ultimate test loads and their corresponding design strengths, calculated according to Eurocode 3 [45], and it was verified that these formulas do not appropriately take into account the thickness of the thicker strap. Similarly, to prevent the risk of brittle failures, such as connection failures or column buckling, Moghimi and Ronagh [46] suggested using diagonal straps that yield and exhibit plastic deformations under high drift ratios. To provide reliable lateral performance under large lateral deformations, they proposed using perforated straps and/or bracket members in four corners of the wall. Placing four C-section cut-offs in the track at the four corners of the frame could also improve the performance of the X-strap system. However, it was shown that the initial slackness in the strap should be as small as possible; otherwise, the strap will fail prematurely at the tension device location.

Fig. 3(j) to (m) show different failure modes of screw connections derived from the study on the maximum load capacity and the load-deformation behaviour of 75 CFS screwed strap bracing connections [29]. It was concluded that the maximum cyclic load was greater than the monotonic load, indicating that the strap bracing material underwent cyclic hardening but with only a small amount of hardening, due to the principal load resistance being through tension. As a result, designing wall bracing systems based on their monotonic capacities is a conservative approach. The work of Davani et al. [47] also demonstrated different types of damage in specimens, such as strap tearing, pulling out of screws, severe distortional buckling of studs, and severe damage in connections, especially frame-to-strap connections, while only strap yielding was considered during the design procedure.

Shake table tests were conducted on two three-storey CFS prototypes, representative of a residential building located in a medium-to-low seismic area [48]. The lateral load-resisting system was designed as a low dissipative seismic structure using strap-braced stud walls with concrete and Oriented Strand Board (OSB) panels. The two prototypes differed only for the type of floors (i.e., composite steel–concrete and wood-based panels). The observed damages were strap yielding and

Table 2
Different types of CFS strap-braced walls sheathed with gypsum board [39].

Shear wall configuration	Types	Bracing type
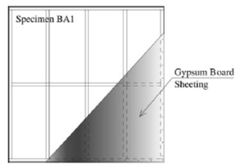	Type 0	----
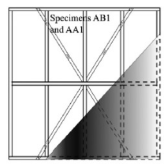	Type I	Strap bracing connected to interior studs and tracks
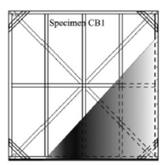	Type II	Strap bracing connected to strong brackets and corners of frame
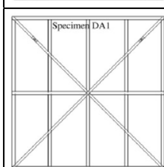	Type III	Strap bracing connected to frame corners
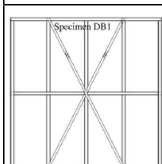	Type IV	Strap bracing connected to interior frame joints
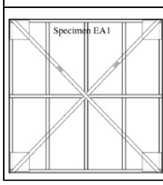	Type V	Strap bracing connected to frame corner with gusset plate

bolt loosening for both concrete and OSB solutions, and local buckling of chord studs for OSB solutions. These two prototypes have been tested on the shake table in another study, in which the CFS strap-braced walls were designed as non-energy-dissipating systems [49]. The collapse mechanism was associated with the local buckling of the tracks in the first-floor walls, while the failure of the diagonal net area at the fastener holes and the yielding of the tension diagonal were the failure modes of the walls in the second and third floors. For structures designed as non-energy-dissipating systems, the seismic response was considered satisfactory. Continuing this project, Landolfo et al. [50] performed an extensive experimental study in three phases (i.e., micro-, meso-, and macro-scale tests) to characterise the seismic behaviour of the two mock-ups investigated in their previous research. Brittle failure mechanisms and the interaction of various phenomenon, such as local buckling of tracks, squashing at stud ends, out-of-plane deformation of gusset plates, and gusset-to-track connection failure, were observed in both monotonic and cyclic tests. In contrast, the observed collapse mechanisms in the shake table test were gusset-to-track connection failure and global buckling of chord studs.

Due to the considerable effect of the corner foundation anchorage details on the lateral strength, stiffness and ductility of the wall systems, enhancing their response is crucial to ensure satisfactory structural performance [33,35,38,40]. To prevent failure due to bending collapse and local buckling of the bottom tracks, the corner details should provide the force transmission from the brace to the anchorage by means of clip angles and hold-downs [51]. Previous studies showed that one angle plate at each chord-to-track connection can be used to transfer the strap load to the support with no bending in the track or track-to-chord failure [39]. The strengthening of the corners is also very important as it has a significant influence on the initial rigidity of the system and their poor design can cause larger in-plane shear deformations than expected as well as premature failure of the braced frame. Referring to [38,40–42], it is recommended that the hold-down detail should be designed in such a way as to carry the probable brace loads with minimal rotation and inelastic damage to the track, chord studs, gusset plate, anchor rod, and hold-down itself. In addition, the corner hold-down plates located in the bottom and top tracks should be designed to provide an adequate capacity to transfer brace induced forces due to the possibility of punching shear failure. Fig. 3(h) and (i) demonstrate the typical track and connection failure modes as well as the punching shear failure mode. In a similar study [46], it was pointed out that hold-downs located inside the frame achieve better performance and strength due to higher punching shear capacity compared to the hold-downs connected to the outer face of the chord members. The use of thicker track sections [38,40–42] and the lower level of eccentricity in the anchor bolt connection with respect to the strap axis [33] can also improve the wall seismic performance.

Table 3
Description of the tested specimens.

Specimen	Description
FP	Flat infill plate specimen with plate thickness of 1.0 mm (20 gauge)
CP	Corrugated infill plate (cold formed steel deck) specimen with plate thickness of 0.75 mm (22 gauge)
B1	Concentrically braced frames with single tube brace and vertical cold-formed steel studs spaced at 457.2 mm (18 in.) centre-to-centre
B2	Concentrically braced frames with single tube brace and without vertical cold-formed steel studs
B3	Concentrically braced frames with solid rectangular X-braces and vertical cold-formed steel studs spaced at 457.2 mm (18 in.) centre-to-centre
B4	Concentrically braced frames with solid rectangular X-braces and without vertical cold-formed steel studs

Although several studies have investigated the response of CFS stud-walls under lateral loads, very few attempts have been devoted to the response of these systems under additional vertical loading. Referring to a study by Moghimi and Ronagh [39], they studied 19 specimens with various configurations as shown in Table 2. It was concluded that if the chord studs can withstand the full load capacity of the straps, then a vertical load equal to 80% of the vertical load capacity of the studs does not affect the lateral capacity of the wall.

With respect to the mixed shear wall systems, it was revealed that the use of diagonal straps could effectively improve the load capacity and stiffness of the CFS shear walls filled with lightweight polymer material (LPM) [52]. A modified strut-and-tie model was also proposed to assist with the design of CFS shear walls filled with LPM. In another study, Liu et al. [53] investigated the performance of CFS walls sheathed with sprayed lightweight mortar and evaluated the impact of adding joint-strengthened knee components or X-shaped steel-strap bracings. The results of their tests revealed greater strength and stiffness, as well as a reduction in crack propagation. Knee elements or steel-strap bracings also enhanced the load-bearing capacity of the specimens while reducing their ductility.

Although non-structural gypsum board improves racking resistance of wall panels and delays the distortional buckling of studs and chords, relying solely on gypsum board cladding may result in brittle failure, according to [39]. In general, the use of gypsum board or bracket members avoids severe pinching in their hysteretic loops due to the plastic slack of strap braces and lack of redundancies. Berman et al. [54] conducted an experimental investigation to compare CFS braced frames and steel plate shear walls in terms of their stiffness, maximum displacement, ductility, cumulative hysteretic energy dissipation, and energy dissipation per cycle for a given strength. The descriptions of the tested specimens are listed in Table 3. According to their findings, braced frames had the highest initial stiffness, while steel plate shear walls with flat infill had the highest ductility, yet both had similar energy dissipated per cycle and cumulative energy dissipation.

In New Zealand, a major research project is underway to develop CFS solutions for medium rise residential apartment buildings up to 6 storeys high, using the high strength cold worked thin gauge steels (i.e., Grade 450 to 550; thickness of 0.95 mm to 1.15 mm). A novel experimental testing rig has been developed that can test two storeys full scale walls under combined cyclic lateral loading and constant vertical loading, representing the demands of earthquake on a load bearing wall that is part of the gravity system. The first set of tests are underway to characterise the performance of CFS strap braced wall panels with yielding strap braces, with combinations of stud thickness, braces on one or both sides, linings on one or both sides. From there the research will progress to determining the performance of wall to floor connections, for platform wall/floor/wall construction and for balloon wall/floor/wall construction. Results will be published from 2023.

2.1.2. Numerical investigations

As a result of the non-linear behaviour of individual components of CFS strap-braced walls and their susceptibility to buckling, numerical modelling of these systems is a challenging task. Although several studies have been conducted to model stud walls sheathed with gypsum panels, OSB panels, glass panels, steel sheets and corrugated steel sheets there is a limitation in the detailed numerical studies on the behaviour of unsheathed strap-braced stud walls.

Several studies have investigated the influence of key design parameters, namely the number of studs, structural element thickness, strap steel grade, and corner connection type, on the seismic performance of strap-braced walls. According to Papargyriou et al. [15], reducing the number of studs did not affect the lateral load capacity of the wall, ductility, and energy dissipation. Regarding the intermediate studs' thickness, it was shown that this parameter did not have a considerable effect on the lateral response of the wall, while the ultimate displacement and the ductility decreased slightly. Although increasing the diagonal strap thickness increases the lateral load capacity and reduces the ultimate displacement of the wall significantly, it leads to higher compressive forces and the failure of the chord studs. It is also worth noting that the chord studs need to be designed for the additional compressive force and moment resulting from the P-Δ effect. By increasing the steel grades, the straps arrive at their ultimate displacement before reaching their ultimate strain. Zeynalian and Ronagh [55] proposed an alternate configuration of strap braced CFS walls where the interior corners were reinforced by brackets to optimize the lateral performance of the walls. In the proposed configuration, the increased bending resistance due to the use of the brackets enhances the capacity of the chords and tracks against buckling. Gerami et al. [56] studied the nonlinear behaviour of strap-braced walls under cyclic and monotonic loading using finite element nonlinear analysis. This investigation was on the basis of a wall specimen with welded connections, taken from the experimental results of a study by Al-Kharat and Rogers [38].

Despite this rather large body of research on the behaviour of the strap-braced walls under lateral loading, very few studies investigated their behaviour under vertical load [15,57] or the influence of multi-hazard interactions, particularly the effect of fire pre-damage on the lateral load resistance of the strap-braced walls [58]. In a study by Papargyriou et al. [15], they found that the lateral load capacity gradually decreased as the vertical load increased beyond a certain limit (i.e., up to 24% drop in lateral load capacity compared to the situation without vertical loading). In a follow-up study, Papargyriou and Hajirasouliha [57] developed a practical design methodology for the seismic design of CFS strap-braced stud wall frames under vertical loading based on the experimentally validated numerical models developed in their previous study [15]. According to their research, the combination of vertical load with the secondary moment due to $P - \Delta$ effect may lead to the premature buckling failure of the chord stud before the full capacity of the straps is exploited.

Regarding the effect of fire on the lateral load resistance of the strap-braced walls, a numerical model of the CFS strap-braced wall was developed to analyse the thermal and structural response of the wall under fire and cyclic horizontal loading (i.e., earthquake or wind) after exposure to fire [58]. The loss of integrity of the gypsum boards and the residual mechanical characteristics of cold-formed steel members resulting from high temperature under fire were found to have the greatest impact on the post-fire response of CFS shear walls. With respect to the failure modes, the ultimate failure of the specimen occurred due to the strap rupture where the strap ties into the frame components, while chord crippling in the back-to-back studs developed immediately above the stiff hold-down bracket.

The "pinching 4" hysteresis curves developed by Lowes et al. [59] are widely applicable for modelling the lateral behaviour of CFS shear walls in OpenSees software. Fiorino et al. [60] designed fourteen buildings with different heights and gravity loads located in three low-to-high seismicity locations according to Eurocodes [45,61]. While the diagonal straps were represented by "truss" elements, the chords were simulated using "elastic beam–column" elements. The "pinching 4" material was assigned to the straps and the "uniaxial elastic" material to the chords. The frames comprised axially elastic "beam–column" elements with pins at the top and bottom, connected to the building through rigid elements. Using a similar modelling approach, Champiche [62] developed numerical models to capture the experimental results of their mock-up tests in terms of dynamic properties, peak roof drift ratios, and peak inter-story drift ratios. While there was a good agreement between experimental and numerical dynamic properties, there was a difference between the experimental and numerical peak inter-story drift and roof drift ratios. The increasing source of deformability due to the rocking phenomenon observed experimentally was identified as the cause of the inaccurate response to high-intensity earthquakes. In a study by Macillo et al. [63], "pinching 4" material was also used to simulate CFS strap-braced stud walls. There was good agreement between the numerical and experimental results in terms of hysteretic force–displacement response curves and energy dissipation.

Non-linear dynamic analysis of a multi-story structure designed using the AISI S213 (2012) [37] was performed by Velchev and Rogers [36] and continued by Comeau et al. [64]. The objectives of these studies were to verify the efficiency of the capacity-based design approach, inter-storey drift limits, seismic force modification factors, and building height limits for such systems. They compared the simpler models with full brace/chord stud models in order to identify the accuracy of the simpler models for the analysis. They pointed out that the simpler models significantly reduced the required computational time, while they provided acceptable results.

High-aspect ratio walls with all-welded gusset plate connections have been studied by Mirzaei et al. [23]. Subsequently, simplified numerical models were developed to determine moment demand in the chord studs by adapting simple truss elements and including tension straps, chord studs, and bottom and top tracks. Carr [65] expressed the hysteretic behaviour of the walls through the "bi-linear with slackness" hysteretic model, which is suitable for diagonally braced systems. This model considers the slackness of the braces which occurs due to their stretch after yield.

2.1.3. Analytical investigations

Macillo et al. [24] presented the outcomes of their research on an "all-steel" design solution in which strap-braced stud walls are the main lateral resisting system. Critical analysis was conducted on the basis of the prescriptions given by the AISI S213 (2009) [66] for CFS structures and the Eurocodes [45,61] for traditional concentrically braced frames. Subsequently, for strap braced CFS structures, seismic design criteria in terms of behaviour factor and capacity design rules have been proposed. In another study, Pastor and Rodríguez-Ferran [67] presented a differential model of the hysteretic behaviour of unsheathed X-braced frames, which can capture the hardening plasticity of diagonal straps under tension and buckling of diagonal straps under compression as well as strength and stiffness degradation. Their model, on the other hand, assumes that the wall is able to maintain its load-carrying capacity despite excessive lateral displacements without ever reaching failure.

Madsen et al. [5] published a report for practising engineers to cover the history of CFS load-bearing and lateral force-resisting systems, construction methods, the design of key elements of such systems, their cyclic performance and the application of ASCE 41 (2014) [68] for these kinds of structural systems. According to this report, since the energy dissipating mechanism in these systems is yielding of the tension straps, the implementation of a capacity-based design for strap-braced wall systems is straightforward. The comparison between the one-sided and double-sided strap-braced walls revealed that the single-sided ones, especially in high aspect ratios, may be subjected to a significant eccentric moment in the chord studs. Hence, both weak-axis and strong-axis bending need to be considered for the expected strength of the strap. The CFS system's cyclic behaviour is highly non-linear, and although pinching is always evident, the force–displacement curves for strap-braced walls do not demonstrate significant strength and stiffness degradation, and therefore, the hysteretic loops are more stable. The typical failure modes and hysteretic behaviour of (i) OSB-sheathed walls; (ii) steel-sheathed walls; and (iii) strap-braced walls are shown in Fig. 6.

2.1.4. Seismic response modification coefficient

The main design parameter that quantifies the inelastic capacity of the structural system is the behaviour factor q (according to the European terminology) or the seismic response modification factor (R) (according to the American terminology). The Applied Technology Council, ATC, first introduced the term "seismic response modification factor" in the ATC-3-06 report [69] released in 1978. The concept of a response modification factor is based on the argument that well-designed structural resistant systems have ductile behaviour and are able to carry large inelastic deformations without collapse. FEMA P-1050 [70] prescribes a seismic response modification factor of 4 for diagonal strap bracing, while UBC [71] specifies an R = 2.8 for this lateral resistance system. According to AS/NZS 4600 (2018) [14], the response modification factor should not be greater than 2 when CFS members are used as the primary earthquake-resistant elements, unless otherwise specified. In USA and Mexico, ASCE 7 (2010) [72] provides a response modification coefficient of 4 for CFS strap-braced stud walls, while in Canada a response modification factor of 2.5 is proposed by NBCC [73]. Eurocode (EN 1998-1) [74] provides capacity design rules for various structural typologies, however, does not provide any capacity design rules and behaviour factors specifically for CFS structures.

The seismic response modification coefficient (R) of braced shear walls has been previously investigated experimentally and numerically in several research studies. Kim et al. [75] used shake table tests to investigate the seismic performance of a full-scale two-storey, one-bay structure braced with straps welded to the flanges of the chord, which was designed in accordance with the TI 809-07 [76]. The dynamic tests revealed a very ductile and highly pinched hysteresis behaviour dominated by the stiffness and yielding of the straps, while a seismic response modification factor (R) of 4 was assumed, which corresponds to the behaviour factor (q) in the European code terminology. According to the results of an experimental study by Fiorino et al. [77], a seismic design method for the design of CFS strap-braced stud walls was suggested. The proposed method was in good agreement with the framework of EN 1998-1 [74]. The seismic force modification factor was found to have values in the range of 2.00 to 2.19. In contrast to the previous study [75], the net section failure of diagonal straps governed the collapse of these walls.

Iuorio et al. [21] compared three different lateral resisting systems made of CFS strap-braced stud walls, which were designed according to elastic or dissipative design approaches to establish some criteria for the seismic design of these systems. In the case of the elastic approach, the wall specimens were located in a medium-low seismicity zone, and a q factor of 1 was considered. The other two groups of walls were designed according to the dissipative approach by considering the behaviour factor q = 2.5 given by AISI S213 (2012) [37] for "limited ductility" and by using the capacity design rules based on the Eurocode approach for traditional steel braced structures. The behaviour factor obtained from the experiments was in the range of 2 to 2.2 for elastic light walls, which was bigger than the behaviour factor adopted in the design phase (q = 1) and proposed by AISI S213 (2012) [37] (q = 1.6) for the "conventional construction" category. Similarly, for the dissipative walls, the test-based behaviour factor (q = 2.5 to 8.2) was higher than the value provided by AISI S213 (2012) [37] in the case of "limited ductility". An opposite conclusion was drawn from the findings of the study by Al-Kharat and Rogers [38,40–42]. Despite using a proposed seismic capacity design approach similar to CSA S16

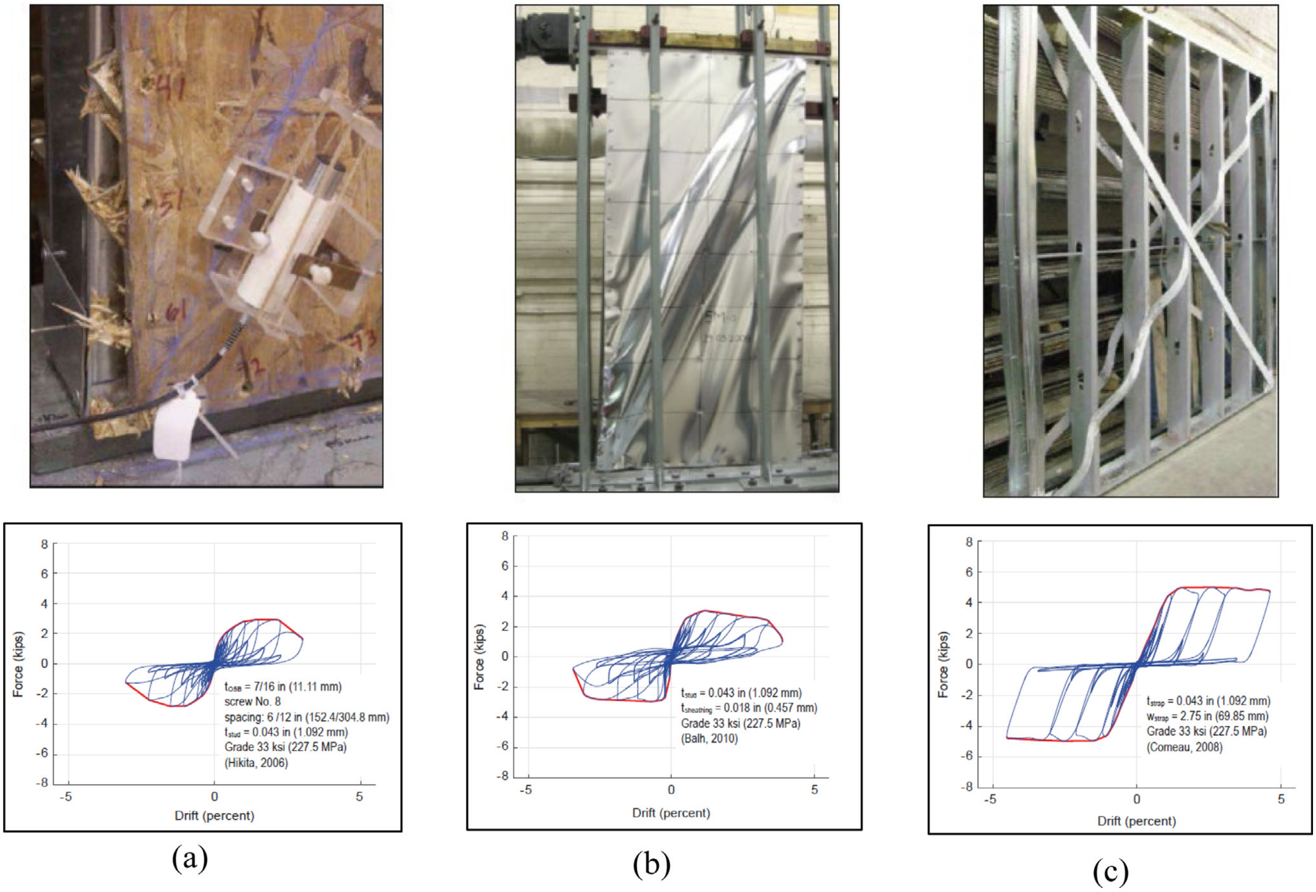

Fig. 6. Failure modes and hysteresis behaviour of (a) OSB-sheathed walls, (b) steel-sheathed walls, and (c) strap-braced walls [5].

(2005) [78], assuming an R factor equal to 4 according to ASCE 7 (2005) [79] for the design of the dissipative walls, behaviour factor values of 3.65, 2.11, and 1.72 were obtained from the experiments. These values indicated attainment of only low ductility levels, which were not compatible with the value of 4 for the *R* factor provided by ASCE 7 (2005) [79]. This response was attributed to the constructive details of the hold-down devices, which in some cases did not allow for reaching or maintaining the strap yield capacity and thus led to a severely overall system ductility reduction. For the elastic approach, they suggested a behaviour factor of 1.6, followed by the AISI S213 (2012) [37] prescription for "conventional construction".

Velchev et al. [25] and Comeau [34] proposed an *R* factor equal to 2.5 for strap-braced walls with welded connections. Based on the test results, *R* factors were evaluated, and minimum and maximum values of 1.6 and 10.4 were obtained, which were greater than those used in the design phase in most cases. Fiorino et al. [60], who expressed a similar value of *R* factor equal to 2.5, investigated a strap-braced wall to define the behaviour factors of CFS strap-braced walls based on FEMA P695 [80] rules. In another study, Abu-Hamd et al. [81] demonstrated that the seismic response modification factor was affected by wall aspect ratio and material yield stress. They pointed out that by using weak braces with sufficient ductility accompanied by strong connections, chord studs, and reinforced track, as well as applying the capacity-based design approach, the *R* factor can be increased for walls with aspect ratios of 1:1 and 1:2. For walls with an aspect ratio of 1:1 and a yield stress of 3.6 MPa and 2.3 MPa, the *R* factor was 5 and 6.2, respectively. On the other hand, walls with an aspect ratio of 1:2 and yield stress of 3.6 MPa and 2.3 MPa had an *R* factor of 5.5 and 5.2, respectively.

2.2. Other types of braced walls

In recent years, extensive research studies have been conducted on the performance of X-strap bracing systems. However, considerably less effort has been devoted to other types of CFS braced walls, namely knee-braced, K-braced and truss-like braced shear walls. As a result, the behaviour of these systems has not been completely understood and appropriate guidelines addressing the seismic design of CFS structures have not yet been fully developed. Therefore, more research work is required to provide a better understanding of the behaviour of these systems and identify their shortcomings in order to cover the lateral design of these systems in detail in the standards of practice.

2.2.1. Experimental investigations

According to a study by Zeynalian and Ronagh [82], the common failure mode of light-weight knee-braced CFS structures was local plastic buckling in the knee-elements to stud connections, followed by rivet pull-out for specimens without brackets. Although these kinds of systems have relatively high maximum drift capacity, their lateral strengths are not as high as X-strap bracing. Therefore, the use of knee- and K-bracing systems is generally limited to the low seismic regions [82,83]. The results revealed that the use of brackets at four interior corners of a wall panel improves the lateral performance of the panel and supports the chords and the tracks against buckling by reducing their buckling length. Fig. 7 shows the bracing configurations and their hysteretic curves [82]. The strength and ductility of the walls can be considerably improved by using washers in the K-elements to stud rivet connections. Furthermore, K-braced elements in the side spans provide higher strength, ductility, and energy dissipation [83].

Table 4
Details of CFS truss-like shear walls.

Shape	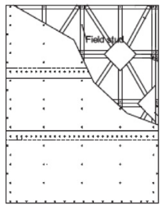			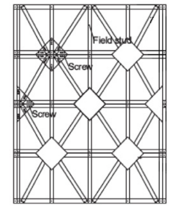	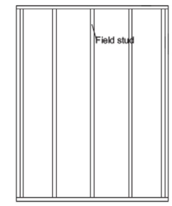
Configuration	1	2	3	4	5
Skeleton construction	Truss	Truss	Truss	Truss	Frame
Sheathing configuration	Corrugated steel sheet	Plain steel sheet	Plain steel sheet	No sheathing	Corrugated steel sheet
Chord studs' type	Built-up section	Built-up section	Back-to-back section	Built-up section	Back-to-back section

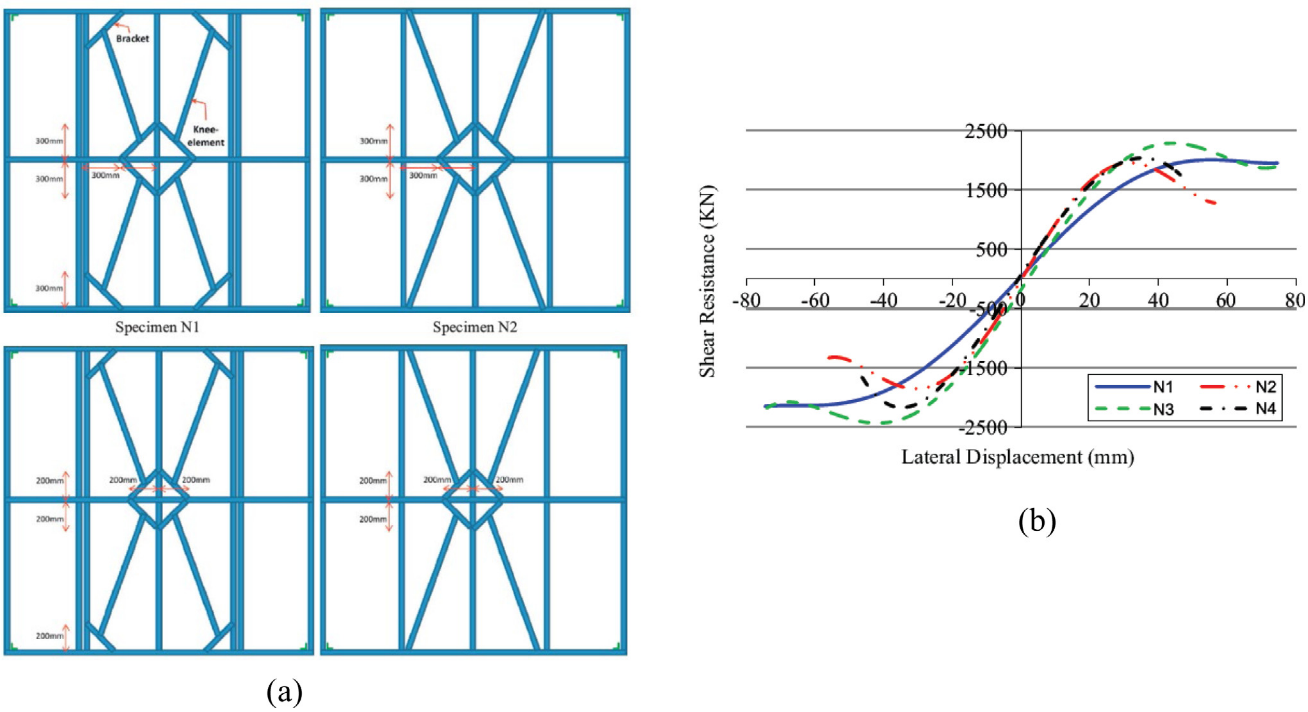

Fig. 7. (a) Different knee bracing configurations, (b) hysteretic envelope curves [82].

In another study, the performance of K-braced CFS shear panels with improved connections has been investigated by Pourabdollah et al. [84]. In general, the dominant failure mode was local buckling in the brace to nogging connections followed by screw pull out and tearing of the brace flanges around the hole. The proper modification of the K-braced connections and the use of gusset plates in the braced to stud connections could significantly increase the shear strength, energy dissipation, and ductility capacities of the K-braced panels.

Tian et al. [85] investigated the behaviour of a novel truss-like shear wall used with various steel sheathing under monotonic and reversed cyclic loading. Details of CFS truss-like shear walls are demonstrated in Table 4. The truss-like shear wall systems provided significantly higher ultimate strength and elastic stiffness and dissipated more energy than the conventional steel-sheathed CFS shear wall systems. A summary of studies on different braced systems is shown in Table A.4 of Appendix A.

2.2.2. Seismic response modification coefficient

Regarding the response modification factor of CFS knee-braced walls, a value in the range of 2.8 to 3.61 has been proposed in the literature [82]. These values show that the suggested R factor of 3 in some design codes such as AISI and FEMA is reasonable, while the prescribed R factor of 2 in the AS/NZS 4600 (2018) [14] seems to be too conservative for the system ductility of well-designed and detailed systems. Furthermore, the R factor is affected by a combination of different structural characteristics and dissipating energy mechanisms. The response modification factor of CFS K-braced walls has been suggested to be a value between 3.3 and 4.3, which implies that the recommended R factors in design standards are relatively conservative for these systems [83]. There is no investigation into the seismic response modification coefficient of truss-like braced shear walls.

2.3. Summary and conclusion

The key findings of the research studies, reviewed in Section 2, in terms of structural performance, are briefly summarised as follows.

2.3.1. Load capacity

The literature review has led to the following main conclusions pertaining to the load capacity of CFS braced shear walls:

- Increasing the braced area enhances the load capacity of the wall panel and provides more room for connections. Furthermore, by increasing the width of the strap, the deflection of a frame

considerably reduces, however, it has little influence on the wall's racking load capacity.
- Using straps on one side of a wall can result in considerable eccentric moments in the chord studs that should be included in their design, as well as a 50% reduction in the maximum load capacity of the walls.
- The stud spacing and change in fuse length have no effect on the lateral performance of the panel.
- Bolted connections are less adequate than screwed connections in terms of strength.
- For the track to chord connections, U profiles provide more capacity for the frames than plates or angles.
- Connecting braces to interior joints provides very good structural performance.
- Hold-downs installed inside the frame acquire better performance and strength due to higher punching shear capacity.
- The strength of the walls can be considerably improved by using washers in the braced to studs' rivet connections.
- Strengthening corner foundation anchorage details is crucial due to their significant impact on the lateral strength of the wall systems.
- Although reinforcing the tracks can provide sufficient compression capacity, their fabrication is very time-consuming, difficult, and uneconomical because of the significant length of reinforcement and the number of screws required to distribute the compression force among the shear anchors.
- Filling the CFS strap-braced walls with lightweight polymer material enhances the load capacity of the CFS shear walls.
- In terms of vertical loads, one study shows that a vertical load equivalent to 80% of the vertical load capacity of the studs has no effect on the lateral capacity of the wall, whereas the other shows a gradual decline in the lateral load capacity as the vertical load increases.
- Other types of braced walls (i.e., K- and knee-bracing systems) should be used only in low seismic zones because their strengths are not as high as X-strap bracing.
- The K-braced elements in the side spans and proper modification of the K-braced connections, along with using gusset plates in the braced to stud connections, provide a significant increase in shear strength.
- The use of double studs does not improve the ultimate strength of these systems.

2.3.2. Stiffness

Despite a rather large body of research on the structural performance of CFS braced shear walls, in terms of lateral load capacity and failure mechanism, less effort has been put into improving their stiffness. Based on the research studies reviewed in Sections 2.1 and 2.2, the following recommendations have been proposed to enhance their stiffness:

- The use of U profiles for the track to chord connections instead of plates or angles
- Increasing the brace area
- Strengthening the corner foundation anchorage details
- Initial tension in the strap braces
- Filling the CFS braced shear walls with lightweight polymer material
- The use of double-stud members as the chords

2.3.3. Ductility and energy dissipation capacity

To attain high ductility and energy dissipation, the braced-walls should be designed using a capacity-based design approach. According to the capacity-based design rules, seismic energy is dissipated through plastic deformation of the net strap cross-sections away from their connections with the chord studs. Some researchers developed a new CFS braced-wall panel in compliance with the capacity-based design principles, allowing energy dissipation of braces through the yielding of a fuse element. According to the literature, walls with aspect ratios closer to one confirm the capacity-based design assumption. Furthermore, the chord studs must be designed to consider weak-axis bending moments in the walls with aspect ratios greater than 1.9:1. The following parameters are shown to affect the ductility and energy dissipation capacity of braced shear walls:

- Use of self-drilling screws accompanied by gusset plates, washers in the braced to stud rivet connections, and strengthening the corner foundation anchorage details can increase the ductility and energy dissipation capacities of braced wall connections.
- Reducing the number of studs does not affect the ductility and energy dissipation capacity of the wall.
- The effective length of the X-bracing is an important component in energy dissipation.
- Higher energy dissipation is provided by K-braced elements in the side spans.

2.3.4. Failure mechanisms

In terms of the failure modes of the braced walls listed in Tables A.1–A.4 in Appendix A, the preferred mechanism of failure of a light-gauge steel braced-wall system to have a ductile seismic performance is generally gross cross-section yielding of the braces. The unfavourable modes of failure, such as damage to the tracks, chord studs, gusset plates, hold-down threaded rods, and net fracture of straps, can prevent the braces from maintaining their yield load; and therefore, the ductility and energy absorption ability of the LFRSs are considerably reduced. The failure load and mechanism are governed by the type of fixity of the strap bracing to the top and bottom plates and the presence of the tensioner unit. Fig. 3 demonstrates the different failure modes of these systems. Despite the numerous measurements that have been proposed in the literature to avoid these undesirable failure modes, they cannot be entirely avoided. To address this issue, the following recommendations are taken from Sections 2.1 and 2.2:

- The use of larger diameters for connecting devices enhances the capacity of connections to exceed the yield stress of the braces, in which connecting devices will be prevented from failing.
- Punching shear failure mode in the tracks can be alleviated by using larger hold-down plates and avoiding locating the corner hold-down plates on the bottom and top tracks, as they cannot provide an adequate transfer of brace-induced forces. Furthermore, by providing the force transmission from the brace to the anchorage by means of clip angles and hold-downs, the bottom tracks are prevented from bending collapse and local buckling.
- The rotation of the corner connections needs to be prevented since it may lead to the moment-induced local buckling of the chord studs on the uplift side of the wall.
- The walls with an extended track typically fail due to strap yielding, whereas walls with a regular track collapse due to track compression or bearing failure.
- The use of flat straps having a reduced width fuse and specimens with reinforced tracks may inhibit the net cross-section failure of braces and lead to bearing failure of tracks.
- The installation of gusset plates or the insertion of hold-downs on the inside of the chords minimises block shear failure of the connection between the braces and the bottom track flanges.
- The use of an angle plate at each chord-to-track connection helps to transfer the brace load to the support with no bending in the track or track-to-chord connection and avoids stud-to-track connection failure.
- Bracket members can be used to reduce the risk of brittle failure modes, such as connection failure, and support the chords and the tracks against buckling by reducing their buckling length.
- A perforated strap can eliminate the brittle failure mode in the CFS braced walls.

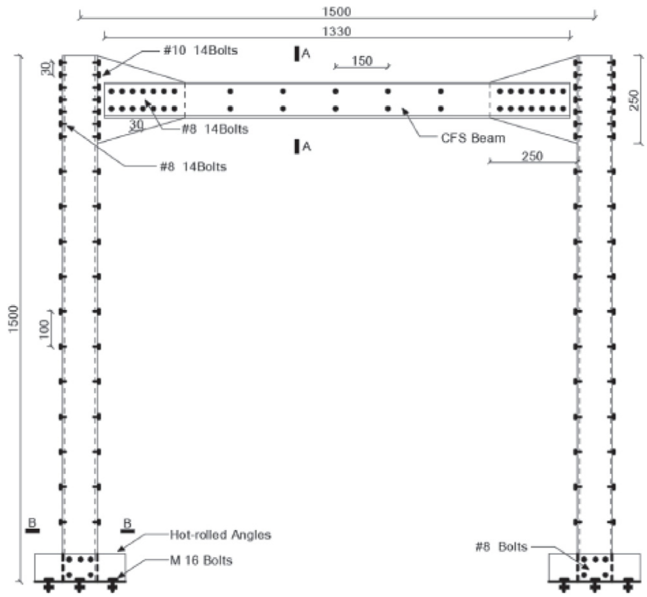

Fig. 8. Frame elevation (All dimensions in mm) [19].

3. Moment resisting frames

Currently, the applications of CFS moment-resisting systems are mainly limited to portal frames and industrial platforms where higher mobility and space-planning flexibility are required. From previous studies, it can be concluded that moment-resisting frames with CFS members generally provide more efficient design solutions in terms of seismic characteristics such as ductility due to their out-of-plane stiffness and energy dissipation compared to conventional CFS shear wall panel systems [86]. The dominant failure mode for CFS bolted moment connections, which was first reported by Lim and Nethercot for channel-sections [3], is characterised by buckling of the web close to the connection zone. The main source of energy dissipation in CFS moment-resisting systems is the inelastic action in the form of bolt slippage and bearing in the bolted moment connection [87]. Therefore, beams and columns are generally designed to remain elastic at the design story drift for the maximum force that can be developed in the connection region [5]. A summary of the studies on moment-resisting frames is provided in Tables B.1–B.3 in Appendix B, based on the adopted research methodologies.

3.1. Experimental investigations

Several experimental studies have been carried out to investigate the effects of key design parameters on the behaviour of moment-resisting frames. Blum and Rasmussen [88] stated that the behaviour of portal frames is sensitive to the strength and stiffness of the connections. While the unbraced frames failed by lateral–torsional buckling of their columns initiated by out-of-plain movement of the knee brace-to-column connection, the frames with braced columns failed due to localised deformations of the apex connection bracket and the rafter at the location of the knee connections. The efficient design of portal frames depends on the design of connections and modifications to connections, including increasing the thicknesses of the bracket and the knee brace. In a follow-up study, it was shown that the initial stiffness and ultimate bending moment capacity increase slightly as the channel thickness increases [89]. Furthermore, changing the channel depth from *C*150 to *C*200 and corresponding apex brackets resulted in an increase in the apex connection stiffness. It was also concluded that the knee-to-column connection is the critical element in the frame, and the frame's ultimate vertical load capacity can be increased by the modification of this connection. Regarding the lateral sway behaviour of CFS frames, Lee et al. [90] concluded that geometrics, joint flexibility, and base conditions are the key parameters affecting the sway stiffness of light steel frames.

The results of the study by Mojtabaei et al. [19] on an innovative CFS moment-resisting frame (see Fig. 8) showed that increasing the axial load ratio of the columns by 50% leads to a decrease of 26%, 62%, and 50% in the ultimate lateral load, energy dissipation capacity, and ductility ratio of the system. Their results indicated that increasing the width-to-thickness ratio of the columns could significantly increase the energy dissipation capacity and ductility ratio of the whole structural system. Other innovative parameters that can influence the behaviour of these frames are curved beam flanges and welded-in vertical beam-stiffeners [86]. These elements enhance the bending moment capacity and ductility by 35% and 75%, respectively, by postponing local buckling failure modes. It was also shown that CFS curved flange beams exceed the nominal plastic moment capacity and sustain this capacity at large rotations. Besides, mobilisation of the bearing action in the connections enables the CFS bolted connections to produce highly stable hysteretic behaviour, which can be used to improve the seismic performance of buildings. However, using CFS curved flange beams may not be very practical considering manufacturing and construction limitations.

The bolt-group in the web of beam elements provides an eccentricity offset from the shear centre of the cross-section, leading to the presence of a bi-moment (warping torsion) which puts each flange into bending about its own plane [3,91]. The bi-moment generates tensile stresses at the top flange/lip junction, opposing the compression stresses due to the major-axis bending moment. As a result, there is an increase in the compression stresses at the top half of the web and a portion of the top flange. This effectively anchors the top flange against distortional buckling and reduces the local buckling critical stress in the web. McCrum et al. [92] also demonstrated that the bi-moment stress component accounted for 41% of the total longitudinal stresses at the section web, implying that the sections would fail at 59% of the design moment. While bi-moment effects can be incorporated into the Direct Strength Method (DSM), disregarding the bolt-group length in the traditional design process can result in nonconservative solutions [91]. The results of the experimental tests conducted by Lim et al. [3] revealed that the strength of bolted moment connections between CFS channel members, where the connections are formed through an array of bolts in the web, is dependent on the length of the bolt-group. For a long bolt-group length, an upper bound would be the full in-plane major-axis moment capacity of the section, which can be predicted using the conventional DSM. The modified DSM, adjusted to include the influence of the bi-moment at the connection, can be used to estimate a reasonable lower bound on the reduced strength for a short bolt-group length in the order of the section depth. In another relevant study, it was demonstrated that the presence of a bimoment induced at the connections in the test frames results in lower ultimate capacities of the tested frames than those obtained using the conventional direct strength method [93]. Moreover, it was found that a frame with a shorter bolt-group length failed at a load approximately 20% lower than that of a frame with a longer bolt-group length [94].

Rinchen and Rasmussen [93] studied the moment–rotation behaviour of different types of connections used in CFS portal frames, including apex, eaves, and base connections. The test results demonstrated that the bending of eaves brackets and the collapse triggered by the fracture of screws dominated the failure modes of eaves connections. The apex connections, on the other hand, failed due to inelastic local buckling around the compression flange-web junction. It was also reported that the base connections exhibited large rotational deformations due to concentrated inelasticity in the connector bracket. In addition, the rigidity of the eaves and apex connections was considerably affected by the bolt tightness and the bracket dimensions [95].

In another study, it was observed that the type of fasteners used to connect the channel lips to the brackets in the apex and eave connections governed the ultimate failure deformation of moment-resisting frames [96]. Dubina et al. [97] also investigated the performance of portal frame eaves and apex joints under monotonic and cyclic loading. They reported bearing elongation of the bolt holes as well as local buckling failure in the beam near to the connection, arising from low overall ductility.

With respect to CFS bolted beam-to-column connections, Wong and Chung [98] investigated the effects of various shapes of gusset plates. As shown in Fig. 9(b) to (e), they identified four different modes of failure: (i) bearing failure in section web around bolt hole; (ii) lateral–torsional buckling of gusset plate; (iii) flexural failure of gusset plate; and (iv) flexural failure of connected cold-formed steel section. They also exhibited the practical feasibility of these connections, which had a moment resistance of 42% to 84% of the bending moment capacity of the beam and proved a semi-rigid response. In another study [20], the structural performance of beam-to-column moment connections has been investigated to facilitate the development of design provisions for a lateral load-resisting system in the AISI S110 [99]. Based on the results, beams and columns should be designed to remain elastic, while energy dissipation capacity should be based on bolt slippage and bearing in moment connections. Yu et al. [100] presented a study to predict the structural behaviour of bolted moment connections between beams and columns and proposed a set of design rules for section failure under combined bending and shear. In addition, beam-to-column bolted connections showed a 34%–88% contribution of the overall frame elastic lateral stiffness for pinned bases and a 17%–33% for rigid base connections [90].

A few research studies investigated the structural performance of moment-resisting frames subjected to gravity and combined gravity and lateral loading conditions. According to Zhang et al. [95], the current AS/NZS 4600 (2018) [14] and AISI S100 (2016) [101] design standards may overestimate the capacity of locally and distortionally buckled portal frames subjected to combinations of horizontal and vertical loads. Another study [96] revealed that the flexural–torsional buckling of columns was the dominant failure mode in the frames subjected to gravity load and combined gravity and lateral load. It was also demonstrated that the joints failed by cross-sectional instability of the beam, triggered by web buckling. It is also worth noting that increasing the thickness of the bracket and the knee brace has a large impact on the frame's ultimate vertical capacity [88]. In a recent study, ShahMohammadi et al. [102] tested their proposed novel cold-formed portal framing system comprising tapered box members formed from two cold-formed nested channel sections under seismic and vertical loading. According to the findings of this study, the frame's failure mechanism under vertical load was concentrated in the deepest section of the rafter adjacent to the knee connection, followed by a significant drop in stiffness (see Fig. 9(j)), while there was a local buckling at the rafter mid-point under cyclic load (see Fig. 9(k)). With respect to the seismic performance of CFS portal frames, McCrum et al. [103] employed true seismic loading using the hybrid test method for the first time. The results showed local buckling in the columns under extreme loading conditions, which needs to be avoided because as it contradicts the strong column–weak beam design philosophy.

The roof sheeting is known to behave as a shear diaphragm under horizontal loads, transferring loads to the end gables. The term "stressed skin" or "diaphragm action" refers to this stiffening effect [104] (see Fig. 10). Wrzesien et al. [104] investigated the effects of joint flexibility and stressed skin diaphragm action on CFS portal frame buildings. The internal frame with roof sheeting resisted nearly three times higher horizontal stress than the bare frame, whereas skin diaphragm action reduced the internal frame's deflection by 90% compared to the bare frame. It is also demonstrated that the joint flexibility of the frame has a significant effect on the load transfer between frames through the roof sheeting, and the true loads transferred to the gable frames are between three and seven times higher than the loads deriving from the tributary area. In a follow-up study, the effect of stressed-skin action on the optimum design of CFS portal frames was investigated using a minimum cost design optimisation [105]. Their findings show that the effect of stress–skin action is greater for buildings with the same span and length (i.e., square-shaped), but reduces as more bays are added (i.e., rectangular-shaped).

The effect of different bolt arrangements on cyclic connection behaviour was investigated by Shahini et al. [107]. They demonstrated that a circular arrangement with slotted holes in the gusset plate can delay local buckling failure in the CFS beam and thus improve the cyclic response. In another study, two novel configurations of CFS moment-resisting joints have been proposed [108]. By postponing the local buckling phenomenon of the connected beams, the new types of connections improved the rotational capacity and energy dissipation capacities of the joints under cyclic load. Although both types of the suggested joints can provide sufficient strength to prevent beam local buckling at the joints, the plastic performance and ductility of the joints need to be improved by providing a better balance between joint strength and connected member slenderness. Tshuma and Dundu [109] developed two configurations for the connection between the rafters and internal columns in the CFS double-bay portal frames, consisting of single channels. Local buckling originating in the compressed portion of the web and spreading to the flanges was identified to be the governing failure mode, as shown in Fig. 9(a).

Teh and Gilbert [110–112] evaluated the accuracy of design equations specified in the AISI (2007) [113] and AS/NZS 4600 (2005) [114] to determine the net section tensile capacity of CFS angles bolted at one angle, flat steel sheets, and channel sections and subsequently proposed more accurate design equations. They demonstrated that the current shear lag factors cause the code equations to predict a greater net section capacity in a bolted connection if the net section area is reduced. Moreover, the shear lag factors calculated using the abovementioned codes often exceed unity and have to be ignored in calculation of the net section tension capacity.

3.2. Numerical investigations

Over the past few years, some research studies have been carried out to investigate the ductility and energy dissipation capacity of CFS moment-resisting connections. Referring to Sato and Uang [106], background information was provided for the development of capacity design provisions in the AISI's first standard for seismic design of CFS moment resisting frames. Fig. 11 shows typical bolted moment connections together with their slip-bearing response. In a follow-up study, Sato and Uang [6,106] presented CFS special bolted moment frames' seismic performance factors such as response modification coefficient, deflection amplification factor, and system overstrength factor.

Using friction-slip is one of the seismic design approaches that is implemented to absorb the energy of the earthquake and consequently reduce and control the damage to the structural elements [86]. Ye et al. [115] investigated the seismic performance of CFS bolted beam-to-column connections with a friction-slip mechanism to obtain more efficient design solutions suitable for CFS frames in seismic regions. According to their results, the friction-slip mechanism provides a horizontal shift in the hysteretic moment–rotation response of the connections, reduces the stress concentrations in the connection zone and postpones the failure of the CFS beam element. Furthermore, using the bolting friction-slip mechanism can significantly improve the energy dissipation capacity and ductility of the CFS bolted connections. In this regard, Bagheri Sabbagh et al. [116] studied the cyclic behaviour of CFS bolted moment connections by considering bolt slip effects. However, the results were limited to the connections with curved-flange beam sections. It was recommended to use non-uniform rotation in the design of such connections, requiring higher bolt pretension. Similarly, Shahini et al. [117] estimated the hysteretic energy dissipation capacity of the CFS connections with circular and square bolting

(a) Local buckling failure [108]

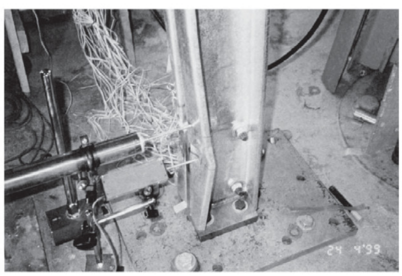

(b) Bearing failure in section web around bolt hole [98]

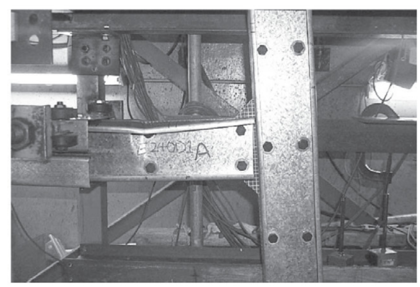

(c) Lateral-torsional buckling of gusset plate [98]

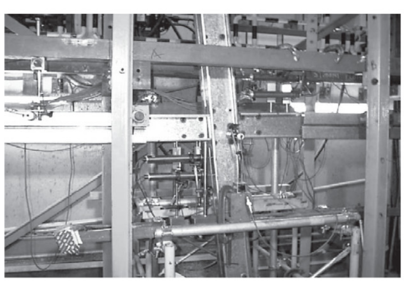

(d) Flexural failure of gusset plate [98]

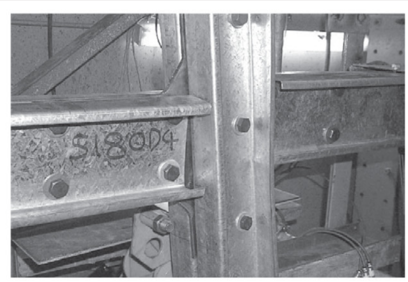

(e) Flexural failure of connected cold-formed steel section [98]

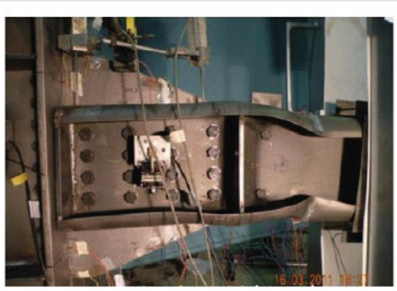

(f) Connection slip and progressive failure [86]

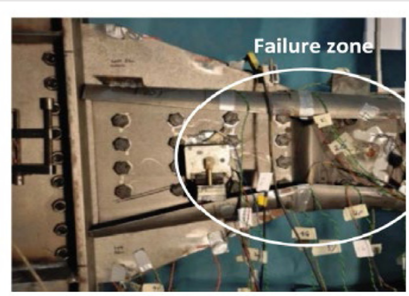

(g) Local/distortional buckling in the CFS beam [120]

Fig. 9. Different failure modes of moment-resisting frames.

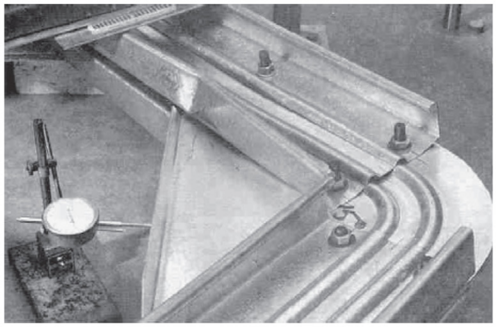

(h) Eaves joint failure [3]

(i) Formation of a spatial plastic mechanism in the flanges and webs [95]

(j) Web and flange buckling in the rafter under vertical load [102]

(k) Local buckling at the rafter mid-point under cyclic load [102]

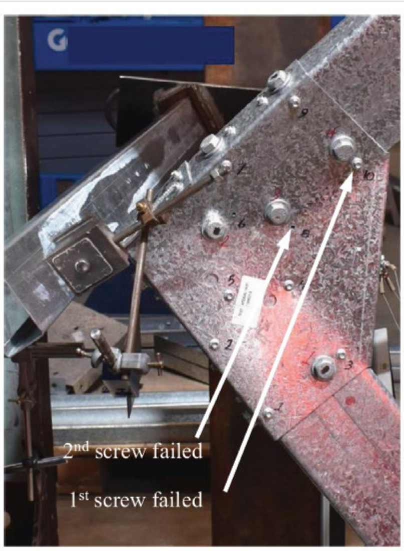

(l) Eaves joint failure [122]

Fig. 9. (*continued*).

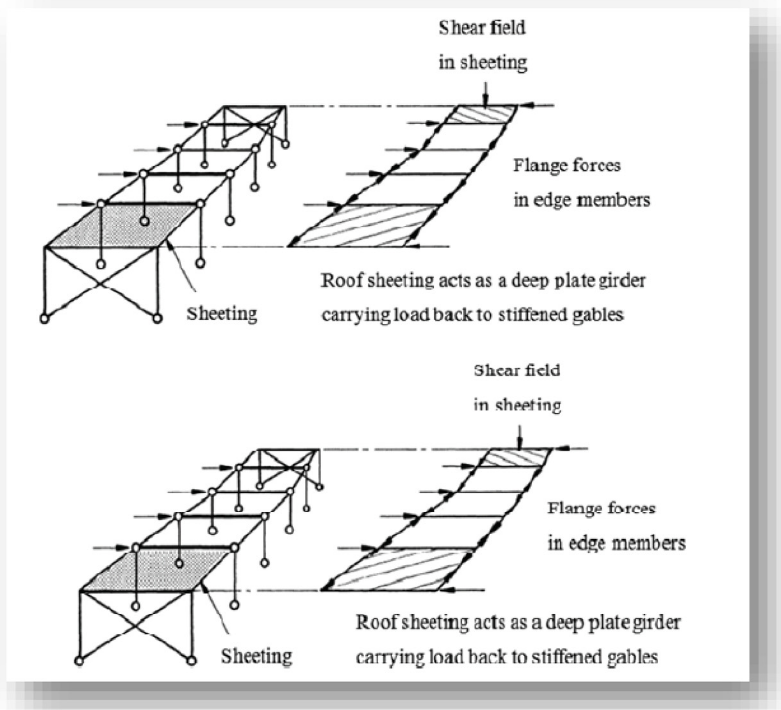

Fig. 10. Stressed-skin action under horizontal load [104].

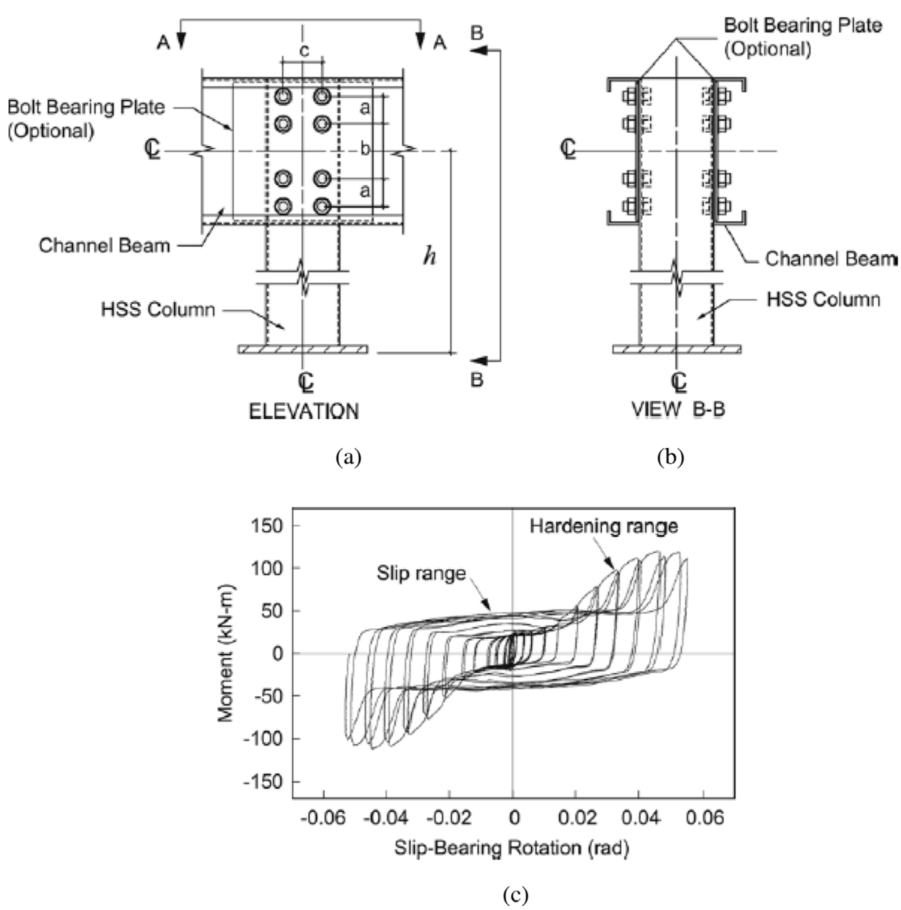

Fig. 11. (a) Typical bolted moment connection detail, (b) typical slip-bearing response of bolted moment [106].

arrangements designed to slip at a specific value. It was concluded that the bolting friction mechanism could effectively eliminate or delay local buckling in CFS beams and significantly improve ductility and energy dissipation capacity due to eliminating the strength degradation and the slackening effect in the hysteretic curves.

Some numerical studies have been conducted to investigate the effects of the cross-sectional configurations and connection types on the seismic performance of the moment-resisting frames. Bagheri Sabbagh et al. [118] pointed out that using CFS beam elements with curved flange can delay local buckling failure modes and provide a more ductile behaviour. In another relevant study, the effects of increasing the number of beam flange bends and different configurations of CFS beam-to-column connections using plates were investigated [119]. The results identified a minimum of two pairs of vertical stiffeners as essential in the connection region to delay web and flange buckling and produce relatively high moment strength and ductility. Furthermore, out-of-plane stiffeners were shown to increase the seismic energy dissipation capacity by up to 90%, the moment strength by up to 35%, and the ductility by up to 75%. A similar conclusion was made by Ye et al. [120], who also investigated the structural behaviour of CFS bolted beam-to-column connections with gusset plates and curved and folded flange channels. They also concluded that the folded flange beam sections create an in-plane stiffness through arching action and can shift the local buckling failure to the web. Furthermore, folded flange beam sections with diamond and circle bolt arrangements were shown to significantly increase ductility and energy dissipation capacity of the connections. A premature failure mode in the gusset plate resulted from using gusset plates with the same or lower thickness than the CFS beam.

In most practical applications, the CFS beam-to-column connections transfer the loads through the web of the beam using a gusset plate while leaving the flanges unattached. In a more recent study, Papargyriou et al. [121] developed two novel CFS beam-to-column connection configurations for seismic applications, which engaged the flanges in the connection behaviour. The cyclic analysis of their proposed web-connected, flange-connected, and web-and-flange-connected connections proved that they were all suitable for practical seismic applications due to their adequate level of ductility while developing more than 80% of the flexural capacity of the connected beam. For web-and-flange-connected joints, T-shaped gusset plates with thicknesses greater than twice the beam thickness provided the best combination of flexural capacity, rotational stiffness, and rotational capacity. With respect to the connections of portal frames, Pouladi et al. [122] investigated the eaves joints comprised of a single channel section and bracket connected through both screws and bolts, which are commonly used in New Zealand and Australia. Although the screws are only used to prevent joint slip during frame erection, the results show that they control the stiffness of the eaves joints since the bolts did not engage in the first screws' failure. Fig. 9(l) shows the shear failure of screws.

Lim and Nethercot [94] presented a simple linear beam idealisation accounting for the semi rigidity of the joints of a CFS portal frame. In this finite element idealisation, beam elements were employed to idealise the column and rafter members as well as to take into account the finite connection length of the joints. Rotational spring elements were employed to represent the rotational flexibility of the joints. Under rafter load, deflections were categorised into three components using the beam idealisation: (i) deflection due to the flexural stiffness of the column and rafter members; (ii) deflection due to the bolt-hole elongation; and (iii) deflection due to the in-plane bracket deformation. Engineers can analyse and design cold-formed steel portal frames using beam idealisation instead of computationally expensive finite element (FE) shell analysis, including making necessary allowances for connection effects. In a similar study [123], the efficiency of the frame proposed based on the simple beam idealisation was compared to that of an equivalent rigid-jointed frame. It was shown that such frames provide competitive alternatives to conventional rigid jointed hot-rolled steel connections for certain combinations of frame geometry and imposed loading. In a follow-up study [124], a FE solid idealisation of a bolted lap-joint in shear was used to determine elongation stiffness. In the light of a beam idealisation of a CFS bolted-moment connection, spring elements were then used to idealise the rotational flexibility of the bolt-groups resulting from bolt-hole elongation. In another study, Chen et al. [125] proposed design equations that can be used to predict the strength of apex brackets used for CFS portal frames.

Mojtabaei et al. [126] evaluated local buckling failure of moment-resisting bolted connections by considering various design parameters, in particular the shape and thickness of the beam, the bolt-group configuration, and the bolt-group length. It was shown that the effects of the local failure from a complex stress state originating from the transfer of both shear and bending moments through the web can be significantly decreased when a longer bolt-group length is used. Finally, a practical design methodology was proposed, which is applicable to bolted connections in CFS flexural members where failure occurs because of localised buckling in the beam. In a related study, the same investigators [127] studied the behaviour, capacity, and design of CFS moment connections under combined loading (bending, shear, and axial force). The results were then used to develop design equations for the compressive capacity of CFS bolted connections failed by local buckling of the web. It was concluded that the presence of a shear lag effect could significantly reduce the cross-sectional capacity of the connected member subjected only to compression. Although a quadratic interaction equation was proposed for the case of combined bending and shear, it was found that the interaction of axial compression with bending and shear can be far more detrimental; and therefore, a linear interaction was presented.

According to the literature, the ultimate moment capacity of bolted moment connections is affected by premature web-buckling, which is sensitive to the length of the bolt-group. However, the findings of a study by Lim and Young [128] pointed out that the value of the ultimate moment capacity at elevated temperatures is controlled by the Young's modulus and yield stress rather than the value of bolt-group length.

3.3. Analytical investigations

Several investigations have been conducted to obtain the optimal design solutions for CFS frames. Mojtabaei et al. [129] presented an optimisation framework to develop CFS bolted moment connections with enhanced energy dissipation capacity and ductility by optimising the cross-sectional shapes of the CFS beam element. It was concluded that for a given plate width and thickness, the optimisation framework results in a considerable improvement in the energy dissipation capacity and ductility of the CFS bolted moment connections. In another study [130], Big Bang-Big Crunch (BB-BC) algorithm was adopted to obtain optimum CFS beam sections at serviceability limit state (SLS) and ultimate limit state (ULS) conditions. The results indicated that the flexural capacity and stiffness of optimum CFS beams could be increased by up to 58% and 44%, respectively, compared to their standard counterparts for the same amount of material. Referring to Wrzesien et al. [131], they investigated the interaction between the rotational arrangement and finite connection length of the eaves joint and proposed the optimum joint detail, in which the size of the brackets is the key parameter of interest under different load combinations and constraints.

The above-mentioned studies were limited to element level optimisation. However, there is an available study coupling the element and structural level optimisation for the design of CFS portal frames [132]. A range of element length, plate thickness and coil width were optimised at element level under different uniformly distributed load levels to maximise their flexural strength. At the structural level, a long-span CFS portal frame with knee braces subjected to different design load combinations was first analysed to determine the elements' internal forces and lateral displacement of the joints. Then, the Genetic

Algorithm (GA) was adopted to find the best design solution by using both optimum and standard CFS sections. It was concluded that the proposed coupled framework could considerably reduce (up to 20%) the required structural weight of the CFS frame system by using the CFS optimised sections compared to the standard sections. In the structural level optimisation, ShahMohammadi et al. [133] developed an optimisation framework to optimise the weight of a novel steel portal frame system, in which cold-formed nested tapered box members were used. The findings show that the novel portal frame system is economically viable, with the added benefit of bird and dust proofing.

Several studies have investigated the tensile behaviour of eccentric bolted CFS connections, considering shear lag effects. Early work in this area was conducted by Munse and Chesson [134] on bolted and riveted tension members, in which the efficiency of a connection was expressed in terms of the net section area, an efficiency coefficient, a fabrication factor, a bearing factor, a shear lag factor, and a ductility factor. Then, all of these factors were used in an empirical design rule for tension connections.

Phan et al. [135] presented an alternative analytical design approach using the Eurocode 3 [136] effective width method to determine the ultimate flexural strength of CFS bolted moment connections by considering bimoment effects. It was shown that while a short bolt-group length may lead to up to a 25% reduction in the flexural strength of the CFS bolted connections, a longer bolt-group length generally results in a moment capacity almost equal to the flexural strength of the CFS channel section.

3.4. Seismic response modification coefficient

Despite several research studies on the seismic response modification coefficient (R) of braced shear walls, very few studies have investigated this factor in the design of moment-resisting frames. Only a value of 3.5 has been proposed based on the large ductility capacity observed from the cyclic testing of beam–column subassemblies [6,106].

3.5. Summary and conclusion

When compared to traditional CFS shear wall panel systems, moment-resisting frames were shown to provide a more efficient design solution in terms of seismic characteristics such as ductility and energy dissipation. However, more research into the non-linear seismic performance of CFS moment-resisting frames with various types of connections and design parameters is needed. The following is a concise summary of the major conclusions of the studies in this section.

3.5.1. Load capacity

The following characteristics reduce the capacity of the moment-resisting frames:

- Increasing the axial load ratio of the columns can cause a reduction of up to 50% in the ultimate lateral load of moment-resisting frames.
- The ultimate capacity of the CFS moment-resisting frames is decreased by the presence of a bimoment induced at the connections.
- The presence of a shear lag effect leads to a significant reduction in the cross-sectional capacity of the connected member.

Several measurements can be taken into account to increase the capacity of moment-resisting frames:

- CFS curved flange beams, increasing the channel thickness, and using a minimum of two pairs of vertical stiffeners in the connection region, can increase the bending moment capacity of the CFS moment-resisting frames.
- Increasing the thickness of the brackets and the knee braces have a significant impact on the frame's ultimate vertical load capacity.
- CFS beam-to-column connection configurations engaging the flanges of the beam in the connection behaviour provide an increase in the flexural capacity of the connected beam.
- The bolt-group length is a determining factor in the flexural strength of the CFS bolted connections, with a moment capacity almost equal to the flexural strength of the CFS channel section at a longer bolt-group length.
- For web-and-flange-connected joints, T-shaped gusset plates with thicknesses larger than double the beam thickness provide the best combination of flexural and rotational capability.

3.5.2. Stiffness

- The initial stiffness of the moment-resisting frame increases as the channel thickness increases.
- By changing the channel depth, the apex connection stiffness is enhanced.
- The bolt tightness and the bracket dimensions have a considerable impact on the rigidity of the eaves and apex connections.
- Sway stiffness can be affected by geometrics, joint flexibility, and base conditions.
- While beam-to-column bolted connections contributed 34%–88% of the overall frame elastic lateral stiffness for pinned bases, they only accounted for 17%–33% of the stiffness of rigid base connections.
- For web-and-flange-connected joints, T-shaped gusset plates with thicknesses greater than twice the beam thickness increase the rotational stiffness.

3.5.3. Ductility and energy dissipation capacity

According to the reviewed studies, the ductility and energy dissipation capacity of CFS bolted connections are primarily determined by four factors: (i) material yielding and bearing around the bolt holes; (ii) yielding lines resulting from the buckling of the CFS cross-sectional plates; (iii) bolt distribution and bolt slippage; and (iv) cross-sectional shapes of the CFS beam elements. The following factors lead to improvements in ductility and energy dissipation capacity:

- Considering the friction-slip mechanism
- Increasing the width-to-thickness ratio of the column
- Using out-of-plane stiffeners in CFS beam-to-column connections
- Folded flange beam sections with diamond and circle bolt arrangements
- Engaging the flanges of the beam into the behaviour of beam-to-column connections

3.5.4. Failure mechanisms

A summary of the failure modes of moment-resisting frames is demonstrated in Fig. 9. The following conclusions can be drawn:

- The ultimate failure deformation is determined by the type of fasteners used to connect the channel lips to the brackets in the apex and eave connections.
- Considering the effects of bimoment efficiently anchors the top flange against distortional buckling and lowers the web's local buckling critical stress.
- The use of curved and folded beam flanges, as well as welded-in vertical beam-stiffeners, delays local buckling failure.
- Frames with unbraced-columns generally fail due to lateral–torsional buckling of the column caused by out-of-plain movement of the knee brace-to-column connection, whereas those with

braced-columns mainly fail due to localised deformations of the apex connection bracket and the rafter at the location of the knee connections.
- In CFS beams, the bolting friction mechanism can prevent or delay local buckling.
- Using two pairs of vertical stiffeners in the connection zone is an efficient method to prevent web and flange buckling in CFS beams.
- Premature failure can be generally avoided by using gusset plates of the same or lower thickness as the CFS beam.
- A longer bolt-group length leads to an extreme decrease in the effects of the local failure from a complex stress state originating from the transmission of both shear and bending moments through the web.

4. Summary and future directions

Despite a significant increase in worldwide demand for lightweight braced structures, the conventional bracing methods are not capable of economically resisting the high lateral demands imposed on the system in high seismic regions or high wind areas. One of the most important and challenging issues is the seismic design of lateral force-resisting systems for such buildings. To address the increased demand and provide reliable and highly economical design solutions, understanding the structural behaviour of CFS systems under extreme load conditions is of significant importance. The emphasis of this paper is to summarise and review the major research developments in order to identify the challenges in the braced-walls and moment-resisting systems. Over 130 studies have been thoroughly examined since 1986, with categories depending on the resisting systems and research approaches. Tables C.1 and C.2 in Appendix C present an overview of the research highlights of the papers reviewed in this study. For future research, effort could be put into developing the following knowledge gaps:

- Demountability and reuse of structures rather than landfilling or recycling them contribute to the reduction of the environmental impact of the built environment by minimising material production and associated carbon emissions. Although CFS structures are well suited to reuse, no studies were found to investigate the demountability and reuse of these systems. Demountable LRFSs would promote the end-of-life scenario of reuse of CFS structural elements.
- The New Zealand braced-walls concept is similar to that being developed overseas. Nonetheless, the higher strength and thinner gauge materials used in this country will cause differences in component and system behaviour. Therefore, more investigation is needed to study the effect of the high strength and thin gauge materials on the seismic behaviour of the CFS strap-braced walls.
- The favourable mechanism of failure of a light-gauge steel braced-wall system in terms of ductile seismic performance is generally gross cross-section yielding of the braces. Although several measures have been proposed in the literature to avoid the undesirable failure modes, they cannot be entirely avoided. It is recommended that future research studies focus on determining comprehensive measurements to completely prevent the unfavourable modes of failure in CFS structural systems.
- Despite the rather large body of research on the behaviour of braced shear walls, no studies could be found on their optimisation. This can be attributed to the fact that the optimisation of such systems can be a challenging task due to typical manufacturing and end-use design constraints, as well as the complicated behaviour of CFS components caused by a combination of local, global, and distortional buckling modes. It is recommended to focus on (i) developing an optimisation framework for obtaining the optimum arrangement of the braced-walls based on their seismic performance characteristics and practical considerations and (ii) presenting an optimum performance-based design methodology for using such braced panels in CFS multi-story buildings.
- Very few studies have been conducted on the response of these systems under vertical loading, combined vertical loading or the influence of fire for example fire following earthquake. Hence, more efforts should be put into better understanding the behaviour of CFS braced walls subjected to these loading conditions. The results of such studies could allow the development of fire-resistant CFS systems and increase their sustainability.
- There are no experimental-based results to investigate the behaviour factor (q) or response modification factor (R) for CFS strap-braced stud walls for multi-storey buildings. Furthermore, as can be seen, different design standards are in disagreement on this factor especially for short buildings. It is also worth noting that there is almost no research on this factor for moment-resisting frames.
- Although some studies have investigated the implementation of the bolting friction-slip mechanism to absorb the energy of an earthquake, there is a lack of research containing different beam section shapes in this field. There is also no design procedure available for such connection systems.
- Despite a rather large body of research on the one-storey CFS moment-resisting frames, there is a need to develop the use of these frames in multi-storey buildings. Furthermore, further studies need to be done to enhance the efficiency and strength of the column members suitable for multi-storey buildings, especially in seismic regions.
- Regarding the moment-resisting frames, considerably fewer research studies have been conducted on the optimisation of CFS structural systems or the simultaneous optimisation of cross-sectional dimensions and the geometry of the whole CFS structural system.
- Only individual fasteners such as bolts, screws, rivets, and welds are covered in the CFS design codes [14,45,101]. The absence of research into the actual CFS connection is one of the main reasons why CFS moment-resisting connections have not been incorporated into the design codes.
- Moment-resisting frames can provide more efficient design solutions in terms of seismic characteristics such as ductility, due to their out-of-plane stiffness and energy dissipation capacity compared to the conventional CFS shear wall panel systems. However, the non-linear seismic performance of CFS moment-resisting frames using different types of connections and design parameters requires more investigation.

CRediT authorship contribution statement

Maryam Hasanali: Writing – original draft, Resources, Project administration, Methodology, Investigation, Data curation, Conceptualization. **Krishanu Roy:** Writing – review & editing, Supervision, Data curation, Conceptualization. **Seyed Mohammad Mojtabaei:** Writing – review & editing, Supervision. **Iman Hajirasouliha:** Writing – review & editing, Supervision, Data curation, Conceptualization. **G. Charles Clifton:** Writing – review & editing, Supervision. **James B.P. Lim:** Writing – review & editing, Supervision.

Declaration of competing interest

The authors declare that they have no known competing financial interests or personal relationships that could have appeared to influence the work reported in this paper.

Data availability

No data was used for the research described in the article.

Appendix A

The major research developments in CFS braced-wall systems are summarised in Tables A.1–A.4.
* Blank cells in all tables show that the reference paper has not specified that feature.

Table A.1
A summary of published experimental literature on strap-braced shear walls.

Researcher	Year	Research methodology	Loading protocol	Scale	Connection type	Failure mechanism
Gad et al. [4]	1999	Experimental	Cyclic racking Dynamic	Full-scale	Screw	1. Strap brace connection failure 2. Tensioner unit 3. Tearing of the plasterboard around the screws 4. Crushing of the plasterboard edges
Iuorio et al. [21]	2014	Experimental Analytical	Cyclic Monotonic	Full-scale	Gusset plate along with screw	1. Tilting of screw 2. Net section failure of strap bracing 3. Pull-out of screw
Mirzaei et al. [23]	2015	Experimental Analytical	Reversed cyclic Monotonic	Full-scale	Gusset plate along with weld or screw	Failure of chord studs due to flexural and elastic distortional buckling
Velchev et al. [25]	2010	Experimental	Reversed cyclic Monotonic	Full-scale	Gusset plate along with weld or screw Weld Screw	1. Yielding of strap 2. Net cross-section fracture of strap 3. Combined axial compression and flexural failure of chord stud
Tian et al. [26]	2003	Experimental Analytical	Monotonic	Full-scale	Screw	1. Overall buckling of the compression chord 2. Bracing rivet failure
Adhem et al. [27]	1990	Experimental	Lateral cyclic	Full-scale	Weld Gusset plate along with screw	1. Stud buckling 2. Net cross failure of a brace 3. Compression failure of a track
Serrette & Ogunfanmi [28]	1996	Experimental	Monotonic	Full-scale	Gusset plate along with wafer head self-drilling/ self-tapping screw	1. Yielding in the tension strap-bracing 2. Pull-through of the screws and 3. breaking of the board at the edges
Zeynalian et al. [29]	2018	Experimental	Cyclic Monotonic	Full-scale	Screw	Bearing, tilting, tear-out, pull-out, pull-over, net section failure
Tremblay et al. [30]	2003	Experimental	Cyclic	Full-scale	Gusset plate connected with a slip-critical bolted	Premature failure at end connections
Kasaeian et al. [31]	2020	Experimental Analytical Numerical	Cyclic	Full-scale	Wafer head self-drilling/ self-tapping screw	1. Strap yield 2. Tension straps' failure and distortion of top track 3. Flange rupture in the lower track 4. Local buckling of top track
Serrette et al. [32]	2007	Experimental	Cyclic Monotonic	Full-scale	Gusset plate along with self-drilling screw	1. Rupture at the edge of the sheathing 2. Screw pull-out
Casafont et al. [33]	2007	Experimental	Cyclic	Full-scale	Bolted joint	Bearing, tilting, pull-out, pull-through, net section failure, shear failure of the connection device, punching, tearing and local buckling
Comeau [34]	2008	Experimental	Reversed cyclic Monotonic	Full-scale	Weld Gusset plate along with weld	1. Heavy wall: Yielding of braces followed by crushing of chord studs, net section fracture 2. Light wall: Full strap yielding with strain hardening
Fiorino et al. [35]	2016	Experimental Analytical	Reversed Cyclic Monotonic	Full-scale	Gusset plate along with hexagonal head self-drilling screw	1. Local buckling of the tracks 2. Squashing of the stud ends 3. Out-of-plane deformation of the gusset plate 4. Gusset-to-track connection failure
Velchev & Rogers [36]	2008	Experimental	Reversed cyclic Monotonic	Full-scale	Self-drilling screw connected directly to the chord or through gusset plate	1. Compression and bearing failure of the bottom track 2. Yielding of braces 3. Net section fracture 4. Block shear failure of flanges of the bottom track
Al-Kharat and Rogers [38]	2007	Experimental	Reversed cyclic Monotonic	Full-scale	Gusset plate along with weld Wafer head screw	1. Failure of or extensive damage to the tracks, chord studs, gusset plates, hold-down threaded rods, straps (due to net section fracture) 2. Punching shear failure depending on the wall configuration

(continued on next page)

Table A.1 (*continued*).

Researcher	Year	Research methodology	Loading protocol	Scale	Connection type	Failure mechanism
Al-Kharat and Rogers [40]	2005	Experimental	Reversed cyclic Monotonic	Full-scale	Weld Self-drilling/ self-tapping screw Gusset plate along with weld or wafer head self-drilling/ self-tapping screw	1. Fracture of the straps at the net cross-section 2. Failure of the anchor rod in tension 3. Connection failure due to pull out of the screws at the track-to-chord connection 4. Bending in the bottom track due to a hold-down rotation 5. Compression failure of the track 6. Local buckling of the chord studs 7. Fracture of a strap due to corner rotation 8. Punching shear failure of the track in all specimens 9. Punching shear failure of the track with compression failure of the gusset plate 10. Moment induced local buckling of the chord studs 11. Local buckling in the gusset plate with corner rotation 12. Pull out of the screws that connect an interior stud to the track
Al-Kharat and Rogers [41]	2008	Experimental	Reversed cyclic Monotonic	Full-scale	Self-drilling/ self-tapping screw Gusset plate along with self-drilling/ self-tapping screw	1. Yielding of braces 2. Net section fracture of braces 3. Compression and bearing of track 4. Wrapping of chord stud 5. Compression and bearing of track
Al-Kharat and Rogers [42]	2006	Experimental	Reversed cyclic Monotonic	Full-scale	Wafer head self-drilling/ self-tapping screw Gusset plate along with wafer head self-drilling/ self-tapping screw	1. Compression and punching failure of the track 2. Bearing failure of the track at the corner rod location 3. Fracture of strap at the net-section 4. Yielding of strap
Casafont et al. Part 1 [43]	2006	Experimental	Cyclic Monotonic	Full-scale	Screw	1. Combination of tilting, bearing, pull out or pull through 2. Tilting and net section failure
Casafont et al. Part 2 [44]	2006	Experimental	Cyclic Monotonic	Full-scale	Bolted joint	1. Combination of tilting, bearing and tearing of the sheets 2. Tilting, bearing and net-section failure
Moghimi & Ronagh [39]	2009	Experimental	Cyclic	Full-scale	Self-drilling screw Bracket along with self-drilling screw	1. Brittle failure 2. Premature distortional buckling of the 3. Left and right stud at earlier stages of the racking displacement
Moghimi and Ronagh [46]	2009	Experimental	Cyclic	Full-scale	Self-drilling screw Bracket along with self-drilling screw	
Davani ei al. [47]	2016	Experimental	Dynamic	Full-scale	Screw	1. Strap tearing 2. Pulling out of screws 3. Severe distortional buckling of studs 4. Severe damage in connection
Terracciano et al. [48]	2018	Experimental	Cyclic Monotonic Dynamic	Reduced scale (1:3)	Gusset plate along with self-piercing screw	1. Local buckling of the tracks in the first-floor walls 2. Failure of the diagonal net area at the fastener holes 3. Yielding of the tension diagonal in the second and third floors
Fiorino et al. [49]	2019	Experimental	Dynamic	Reduced scale (1:3)	Gusset plate along with self-piercing screw	1. Failure of the diagonal net area at the fastener holes' location 2. Local buckling failure of the tracks 3. Yielding of the tension diagonal
Landolfo et al. [50]	2021	Experimental	Reversed cyclic Monotonic Dynamic	Full-scale	Gusset plate along with screw	1. Meso-scale tests: Local buckling of tracks, squashing at stud ends, out-of-plane deformation of gusset plates and gusset-to-track connection failure 2. Macro-scale tests: Gusset-to-track connection failure, global buckling of chord stud
Fülöp & Dubina [51]	2004	Experimental	Cyclic Monotonic	Full-scale	Self-drilling screw	1. Yielding in the brace 2. Unexpected failure of the corners

(*continued on next page*)

Table A.1 (*continued*).

Researcher	Year	Research methodology	Loading protocol	Scale	Connection type	Failure mechanism
Wang et al. [52]	2020	Experimental Analytical	Cyclic	Full-scale	Self-drilling screw	1. Distortional buckling in interior stud 2. Local buckling in end stud 3. Tilting of self-drilling screws 4. Crashing and cracking of LPM 5. Bond–slip cracks, 6. Shedding and bulging of gypsum board 7. Diagonal cracks of cement fibre board around self-drilling screws 8. Cracking of gypsum board at opening corner 9. Cracking of rib lath sheathing at opening corner 10. Local buckling in opening edge stud
Liu et al. [53]	2016	Experimental	Cyclic	Full-scale	Gusset plate along with self-drilling screw	1. Local buckling of the connection 2. Screw pull-out 3. Flexural–torsional buckling of the end studs 4. Local buckling of the web 5. Flexural–torsional buckling of the interior studs
Berman et al. [54]	2005	Experimental	Cyclic	Full-scale	Gusset plate along with weld	1. Local buckling 2. Bearing failure of the intermediate studs 3. Fractures of the infill plate at locations of repeated local buckling
Kim et al. [75]	2006	Experimental	Dynamic	Full-scale	Weld	1. Significant yielding in the straps along their entire length 2. Yielding of the columns near the anchors
Fiorino et al. [77]	2016	Experimental Analytical	Cyclic Monotonic	Full-scale	Gusset plate along with self-drilling screw	1. Net-section failure of diagonal straps 2. Brace yielding

Table A.2
A summary of published numerical literature on strap-braced shear walls.

Researcher	Year	Research methodology	Loading protocol	Scale	Connection type	Software	Failure mechanism
Papargyriou et al. [15]	2021	Numerical	Cyclic Monotonic Dynamic	Full-scale	Self-drilling screw	ABAQUS	1. Yielding of the straps 2. Distortional buckling of the chord flanges
Zeynalian and Ronagh [55]	2012	Numerical	Monotonic	Full-scale	Bracket along with wafer head screw	ANSYS	1. Screw pull-out at the strap to frame connection 2. Rivet tilting and hole bearing at the stud members ‘connections 3. Strap yielding 4. Buckling failure of the chords
Gerami et al. [56]	2015	Numerical	Cyclic Monotonic	Full-scale	Gusset plate along with welded connection	MSC PATRAN-NASTRAN	
Papargyriou et al. [57]	2021	Numerical	Cyclic Monotonic Dynamic	Full-scale	Self-drilling screw	ABAQUS	1. Net cross-section fracture of the straps 2. Local bucking at the chord studs 3. Premature failure of chord studs before straps reaching their ultimate capacity because of the development of secondary moment due to the P-Δ effects
Ni et al. [58]	2022	Numerical	Cyclic horizontal Fire	Full-scale	Gusset plate along with fastener	SAFIR	1. Strap buckling 2. Strap rupture 3. Chord crippling

(*continued on next page*)

Table A.2 (*continued*).

Researcher	Year	Research methodology	Loading protocol	Scale	Connection type	Software	Failure mechanism
Fiorino et al. [60]	2017	Numerical	Cyclic Dynamic	Reduced-scale	Screw	OpenSees	1. Chord stud failure due to tension or global buckling
Champiche [62]	2021	Numerical	Cyclic Dynamic	Reduced-scale (1:3)	Gusset plate along with self-drilling screw	OpenSees	
Macillo et al. [63]	2018	Numerical	Cyclic	Reduced-scale	Gusset plate along with screw	OpenSees	1. Yielding of steel straps 2. Net failure of strap connections 3. Buckling of tracks 4. Failure in tension and shear anchors
Comeau et al. [64]	2010	Numerical	Dynamic	Reduced-scale		Ruaumoko	
Carr [65]	2015	Numerical	Cyclic	Reduced-scale		Ruaumoko	
Abu-Hamd et al. [81]	2018	Numerical	Monotonic Dynamic	Full-scale	Gusset plate along with screw	ANSYS	1. Yielding of the brace material 2. Buckling deformation of chord stud

Table A.3
A summary of published analytical literature on strap-braced shear walls.

Researcher	Year	Research methodology	Loading protocol	Scale	Connection type	Failure mechanism
Madsen et al. [5]	2016	Analytical	Cyclic Monotonic Seismic			
Dubina et al. [13]	2012	Analytical				
Sharafi et al. [22]	2018	Analytical				
Macillo et al. [24]	2014	Analytical	Seismic			
Pastor and Rodríguez-Ferran [67]	2005	Analytical	Cyclic Dynamic	Reduced-scale	Self-drilling screw	

Table A.4
A summary of published experimental literature on other configurations of braced shear walls.

Researcher	Year	Research methodology	Loading protocol	Scale	Connection type	Failure mechanism
Zeynalian and Ronagh [82]	2012	Experimental Numerical	Cyclic	Full scale	Bracket along with rivet	Local plastic buckling in the knee-elements to studs connections, followed by rivet pull-out for specimens without bracket
Zeynalian and Ronagh [83]	2012	Experimental Numerical	Cyclic	Full scale	Rivet	Plastic local buckling in the K-elements to studs connections followed by rivet pull-out
Pourabdollah et al. [84]	2017	Experimental	Cyclic	Full-scale	Gusset plate along with self-drilling screw	Local buckling in the brace to nogging connections followed by screw pull out and tearing of the brace flanges around the hole
Tian et al. [85]	2015	Experimental	Cyclic Monotonic	Full-scale	Gusset plate along with screw	1. Wall failure: Sheathing separation from top track, flange local buckling and screw pull-out failure at brace, buckling of chord studs 2. Brace-to-track connection failure: Flange local buckling in top track, distortional buckling in brace flange

Appendix B

The major research developments in CFS moment-resisting frames are summarised in Tables B.1–B.3.
* Blank cells in all tables show that the reference paper has not specified that feature.

Table B.1
A summary of published experimental literature on moment-resisting frames.

Researcher	Year	Research methodology	Loading protocol	Scale	Connection type	Failure mechanism
Lim and Nethercot [3]	2003	Experimental Numerical	Monotonic bending	Full-scale	Gusset plate along with bolt	Cross-sectional instability of the beam, triggered by web buckling
Sato and Uang [6]	2010	Numerical	Seismic	Full-scale	Bolt	Yield like plateau due to bolt slippage and then followed by a significant hardening due to bearing at bolt holes in the moment connection region
Mojtabaei et al. [19]	2018	Experimental Numerical	Monotonic	Full-scale	Gusset plate along with bolt	1. Local damages at the bottom and top of columns 2. Outward deformations in the channels' web 3. Inward deformations in channels' flanges and gusset plates
Uang et al. [20]	2010	Experimental	Cyclic	Full-scale	Bolt	Connection failure Local buckling in the beam or column due to flexure
Bagheri Sabbagh et al. [86]	2012	Experimental	Cyclic	Full-scale	Gusset plate along with bolt	1. Connection slip and progressive failure Web and flange buckling 2. Opened up of the flanges at the end of the beam
Kirk [87]	1986	Experimental	Vertical	Full-scale	Bolt	Buckling of the web, close to the connection zone
Blum and Rasmussen [88]	2019	Experimental	Gravity Combined gravity and lateral	Full-scale	Bracket along with bolts	1. Distortional buckling in columns under vertical load 2. Localised deformations of the apex bracket and of the rafters at the location of the knee connections under vertical load 3. Lateral–torsional buckling in the columns subjected to the combined actions 4. Out-of-plane movement of the knee and bracket under combined loading
Blum and Rasmussen [89]	2019	Experimental Numerical	Gravity Combined gravity and lateral	Full-scale	Bracket along with bolts	1. Lateral–torsional buckling of the column following out-of-plane movement of the bracket 2. Distortional buckling of the rafter near the knee connection under combined loading 3. Distortional buckling of the column under gravity load
Lee et al. [90]	2017	Experimental	Vertical	Full-scale	Bolt	Flange cleat or column flange in bending
Lim et al. [91]	2004	Experimental	Monotonic bending	Full-scale	Gusset plate along with bolt	Cross-sectional instability of the beam, triggered by web buckling
McCrum et al. [92]	2019	Experimental	Cyclic	Full-scale	Gusset plate along with bolt	1. Local web and flange buckling 2. Fracture/tearing along the fold lines 3. Fracture of steel in the smaller sections
Lim and Nethercot [94]	2004	Experimental Numerical	Monotonic bending	Full-scale	Gusset plate along with bolt	
Rinchen and Rasmussen [93]	2019	Experimental Numerical	Incremental horizontal force	Full-scale	Gusset plate along with bolt Self-drilling Tek screws	1. Twisting of left and right C-sections near the eaves bracket 2. Bending of C-sections along bolt lines 3. Web buckling of eaves brackets 4. Fracture of screws 5. Tearing of C-section lips
Zhang et al. [95]	2016	Experimental	Combinations of horizontal and vertical loads	Full-scale	Gusset plate along with bolt	1. Local and distortional buckling 2. Formation of a spatial plastic mechanism in the flanges and webs of the one of the columns at a location relatively close to the eave joint 3. Frame failure in a flexural mode in one of the column members near the beam–column connection
Rinchen and Rasmussen [96]	2020	Experimental	Gravity Combined gravity and lateral	Full-scale	Bracket along with bolts	1. Twisting of both columns in the direction opposite to each other besides the horizontal displacements 2. Flexural–torsional buckling of columns

(continued on next page)

Table B.1 (*continued*).

Researcher	Year	Research methodology	Loading protocol	Scale	Connection type	Failure mechanism
Dubina et al. [97]	2009	Experimental	Cyclic Monotonic	Full-scale	Gusset plate along with bolt	1. Bearing elongations of the bolt holes 2. Local buckling failure in the beam adjacent to the connection
Wong and Chung [98]	2002	Experimental	Lateral	Full-scale	Bolt Gusset plate along with bolt	1. Bearing failure in section web around bolt hole 2. Lateral–torsional buckling of gusset plate 3. Flexural failure of gusset plate 4. Flexural failure of connected cold-formed steel section
Yu et al. [100]	2005	Experimental Analytical	Horizontal	Full-scale	Gusset plate along with bolt	Flexural failure of connected sections
ShahMohammadi et al. [102]	2022	Experimental	Seismic Vertical	Full-scale	Gusset plate along with bolt	1. Failure in deepest section of the rafter adjacent to the knee connection 2. Web local buckling 3. Flange local buckling
McCrum et al. [103]	2020	Experimental	Hybrid seismic	Full-scale	Gusset plate along with bolt	Local buckling of the column
Wrzesien et al. [104]	2015	Experimental	Vertical Horizontal	Full-scale	Gusset plate along with bolt	1. A combination of end sheet-to-purlin connection failure and seam failure 2. Failure of the roof panels together with severe deformations of the purlins
Shahini et al. [107]	2018	Experimental Numerical	Cyclic	Full-scale	Gusset plate along with bolt	
Yin et al. [108]	2022	Experimental	Cyclic Monotonic	Full-scale	Gusset plate along with bolt	1. Buckling of the beam flange and web adjacent to the joint area 2. Cracks on the beam flange 3. Buckling of the beam flange and web at the edge of the joint area 4. Cutting of the first bolt on the upper side of the column
Tshuma and Dundu [109]	2017	Experimental	Vertical	Full-scale	Bolt	1. Local buckling in the compression zone of the web and flange of the channels 2. Bearing distortion of bolt-holes
Teh and Gilbert [110]	2013	Experimental	Tension	Full-scale	Bolt	1. Net section failure 2. Bearing
Teh and Gilbert [111]	2013	Experimental	Tension	Full-scale	Bolt	3. Tilt bearing
Teh and Gilbert [112]	2012	Experimental	Tension	Full-scale	Bolt	

Table B.2
A summary of published numerical literature on moment-resisting frames.

Researcher	Year	Research methodology	Loading protocol	Scale	Connection type	Software	Failure mechanism
Ye et al. [115]	2019	Numerical	Cyclic Monotonic	Full-scale	Gusset plate along with bolt	ABAQUS	Local buckling of the CFS beam section close to the first row of the bolts
Bagheri Sabbagh et al. [116]	2013	Numerical	Cyclic	Full-scale	Gusset plate along with bolt	ABAQUS	1. Deformation in the beam 2. Slip in connections 3. Global rotation
Shahini et al. [117]	2013	Numerical	Cyclic Monotonic	Full-scale	Gusset plate along with bolt	ABAQUS	1. Unfavourable local buckling failure 2. Premature flange local buckling
Bagheri Sabbagh et al. [118]	2011	Numerical	Seismic	Full-scale	Gusset plate along with bolt	ABAQUS	Local buckling of the flange accompanied by web buckling
Bagheri Sabbagh et al. [119]	2012	Numerical	Seismic	Full-scale	Gusset plate along with bolt	ABAQUS	Web buckling at the end of the through plate
Ye et al. [120]	2020	Numerical	Cyclic Monotonic	Full-scale	Gusset plate along with bolt	ABAQUS	Local buckling of the CFS beam section close to the first row of the bolts

(*continued on next page*)

Table B.2 (*continued*).

Researcher	Year	Research methodology	Loading protocol	Scale	Connection type	Software	Failure mechanism
Papargyriou et al. [121]	2022	Numerical	Cyclic Monotonic	Full-scale	Gusset plate along with bolt	ABAQUS	Local buckling of the beam web, followed by buckling of the compression flange
Pouladi et al. [122]	2019	Numerical	Combination of moment, axial and shear loas	Full-scale	Bracket along with screw and bolt	ABAQUS	1. Shear failure of screws 2. Twisting of the channel sections 3. Formation of a yield line in the bracket
Lim and Nethercot [123]	2002	Numerical	Bending	Full-scale	Gusset plate along with bolt	ABAQUS	
Lim and Nethercot [124]	2003	Numerical	Bending	Full-scale	Gusset plate along with bolt	ABAQUS	Premature failure of the channel section
Chen et al. [125]	2021	Numerical	Vertical load	Full-scale	Gusset plate along with bolt	ABAQUS	Buckling of the apex brackets
Mojtabaei et al. [126]	2020	Numerical	Compression, bending and shear	Full-scale	Gusset plate along with bolt	ABAQUS	Local buckling of the web
Mojtabaei et al. [127]	2021	Numerical	Compression, bending and shear	Full-scale	Bolt	ABAQUS	Local buckling of the web
Lim and Young [128]	2006	Numerical	Bending	Full-scale	Bolt	ABAQUS	Premature web buckling failure

Table B.3
A summary of published analytical literature on moment-resisting frames.

Researcher	Year	Research methodology	Loading protocol	Scale	Connection type	Failure mechanism
Wrzesien et al. [105]	2016	Analytical	Vertical Wind	Full-scale	Gusset plate along with bolt	
Sato and Uang [106]	2009	Analytical	Seismic	Full-scale	Bolt	
Mojtabaei et al. [129]	2021	Analytical Numerical	Seismic	Full-scale	Gusset plate along with bolt	Local buckling in the beam web close to the connection zone
Mojtabaei et al. [130]	2019	Analytical Numerical	Bending	Full-scale	Bolt	Local and distortional buckling
Wrzesien et al. [131]	2012	Analytical Numerical	Vertical Wind	Full-scale	Gusset plate along with bolt	
Phan et al. [132]	2020	Analytical	Vertical Wind	Full-scale	Gusset plate along with bolt	
ShahMohammadi et al. [133]	2017	Analytical Experimental	Seismic Vertical	Full-scale	Gusset plate along with bolt	
Munse and Chesson [134]	1963	Analytical			Bolt	
Phan et al. [135]	2020	Analytical	Bending	Full-scale	Bolt	Local buckling of the web

Appendix C

See Tables C.1 and C.2.

Table C.1
A summary of research highlights on braced walls.

Researcher	Research highlights
Gad et al. [4]	Tearing of the strap at strap-to-frame connection can be avoided by using: (i) a perforated strap. (ii) a solid strap with sufficient ratio of ultimate to yielding stress. (iii) brackets or gusset plates.
Madsen et al. [5]	A significant eccentric moment in the chord studs in the single-sided strap-braced walls.
Dubina et al. [13]	Introducing two different methods to design CFS members against seismic actions: the “sheathing-braced” and the “all-steel” approach.
Papargyriou et al. [15]	Developing a practical design methodology for the seismic design of CFS strap-braced stud wall frames under vertical loading.
Iuorio et al. [21]	For both elastic and dissipative walls, the test-based behaviour factor was higher than the value given by AISI S213.
Sharafi et al. [22]	A summary of recent research in the field of lightweight steel frame lateral load resisting capacity.
Macillo et al. [24]	Proposing the seismic design criteria for strap-braced walls in terms of behaviour factor and capacity design rules
Tian et al. [26]	1. A 50% reduction in the maximum load capacity of single-sided strap braced walls. 2. Obtaining the best racking performance by using frames with 2-sided X-straps. 3. Little influence of the cross-sectional area of a strap on the racking load capacity, while significant influence on the deflection of a frame.
Adhem et al. [27]	Enhancing the load capacity of the wall panel and reducing its deflection by increasing the strap area.
Serrette and Ogunfanmi [28]	Using wider straps to increase the lateral resistance and stiffness of strap-braced walls.
Serrette et al. [32]	A brace force greater than the minimum specified value of strap yield strength for the design of chord studs, tracks, and frame-to-strap connections.
Mirzaei et al. [23] Velchev et al. [25] Comeau [34]	1. Confirmation of the capacity-based design assumption for walls with aspect ratios closer to 1. 2. A more ductile behaviour in walls with aspect ratios of 1:1 and 2:1 as opposed to those with a 4:1 aspect ratio. 3. A significant moment in the chord studs at the location of the strap connection in strap-braced walls with high aspect ratios. 4. Examine the welded strap braced walls.
Zeynalian et al. [29]	1. Thicker straps have a greater carrying capacity. 2. It is a conservative approach to design wall bracing systems to the monotonic capacities.
Tremblay et al. [30]	The use of effective length of the braces to determine their compression strength and to characterise their hysteretic response, including energy dissipation capability.
Kasaeian et al. [31]	1. Lower ductile behaviour for the straps by increasing the thickness and strength of strap braces. 2. No considerable influence on the lateral performance of the panel by change in the stud spacing and length of the fuse.
Casafont et al. [33]	1. Net section failure of the diagonal strap after yielding is the preferred failure mode. 2. The strengthening of the corner foundation anchorage is crucial. 3. Obtaining ductile behaviour and dissipation capacity of the walls through the use of a lower steel grade for the straps.
Fiorino et al. [35]	1. The effect of wall corners on the overall wall response. 2. Non-ductile seismic performance of the stud wall system as a result of gusset-to-track connection failure.
Velchev and Rogers [36]	1. Considering the capacity-based design approach to achieve high ductility and energy dissipation. 2. The use of gusset plates to prevent the bottom track from buckling.
Al-Kharat and Rogers [38,40–42]	1. Improved inelastic performance of CFS braced walls due to the use of thicker track. 2. The use of the larger diameter connecting devices to enhance their capacity higher than the yield stress of the braces. 3. The use of a larger hold-down plate to reduce the possibility of punching shear failure. 4. Preventing corner connection rotation from causing moment-induced local buckling of the chord studs on the uplift side of the wall. 5. The use of extended track to avoid track compression or bearing failure. 6. The use of flat straps with a reduced width fuse and specimens with reinforced tracks to prevent the net cross-section failure of braces as well as compression and bearing failure of tracks. 7. The installation of gusset plates or the insertion of hold-downs on the inside of the chords to minimise block shear failure of the connection. 8. Considering the capacity-based design approach to achieve high ductility and energy dissipation.
Casafont et al. [43,44]	The preferred mode is net section failure of the diagonal strap after yielding, which can be given by: (i) placing enough screw columns in the joint. (ii) connecting two steel sheets of varying thicknesses. (iii) the usage of washers in bolted connections.
Moghimi and Ronagh [39]	1. The use of a single angle plate at each chord-to-track connection to prevent track bending or track-to-chord failure. 2. A vertical load equal to 80% of the vertical load capacity of the studs does not affect the lateral capacity of the wall.
Moghimi and Ronagh [46]	1 To achieve a very good performance by connecting the straps to the interior joints. 2. Increasing punching shear capacity by locating hold-downs inside the frame.
Davani ei al. [47]	1. Using an anchorage system, gusset plate, and bracket at corners to prevent serious damage to the strap-to-frame connections. 2. The use of cladding to enhance the lateral stiffness and strength of the CFS walls.
Fiorino et al. [49]	The seismic response can be considered as satisfactory for structures designed as non-energy-dissipating systems.

(*continued on next page*)

Table C.1 (*continued*).

Researcher	Research highlights
Landolfo et al. [50]	1. The micro-scale tests was used to investigate the design parameters and the local response. 2. The meso-scale test results highlighted the typical problems that occur in case of non-adopting the specific capacity design seismic rules. 3. In macro-scale tests, the rocking phenomenon produced by the significant elongation of the tension anchorages was detected.
Fülöp and Dubina [51]	The force transmission from the brace to the anchorage by means of clip angles and hold-downs.
Wang et al. [52]	The load capacity and stiffness of the CFS shear walls filled with lightweight polymer material can be improved significantly by using diagonal straps.
Liu et al. [53]	1. Knee elements do not considerably improve the shear capacity and lateral stiffness of the wall when compared to X-shaped bracings. 2. Sheathing with sprayed lightweight mortar is used to enhance the performance of shear walls.
Berman et al. [54]	Both steel plate shear walls and braced frames have similar energy dissipation per cycle and cumulative energy dissipation.
Zeynalian and Ronagh [55]	Reinforce the interior corners of the walls by brackets to optimize their lateral performance.
Gerami et al. [56]	1. Using two-sided X-straps to obtain the highest response modification factor. 2. Improving the shear resistance of the walls by increasing the wall height-to-length ratio. 3. 60% more shear resistance in the walls with two-sided X-straps.
Papargyriou et al. [57]	1. The lateral load capacity decreases as the vertical load increases. 2. Reducing the number of studs does not affect the lateral performance of the wall. 3. The thickness of the intermediate studs has no effect on the wall's lateral response, but it does reduce final displacement and ductility.
Ni et al. [58]	1. The cold-formed steel residual mechanical properties can be used to predict the post-fire lateral capacity of the walls using ambient temperature methodologies. 2. The loss of gypsum board integrity, the maximum temperature attained in cold-formed steel members during the fire, and the consequent residual mechanical properties have the largest impact on cold-formed steel shear wall post-fire reaction.
Fiorino et al. [60]	Confirming the suitability of a value of 2.5 for the behaviour factor of CFS strap-braced stud
Champiche [62]	Due to the rocking phenomenon in experiments, numerical and experimental results for high intensity earthquakes are not in good agreement.
Comeau et al. [64]	With aspect ratios of 1:1 and 2:1, the walls show more ductile behaviour.
Carr [65]	The "bi-linear with slackness" hysteretic model was used to express the hysteretic behaviour of the walls.
Pastor and Rodríguez-Ferran [67]	A differential model of the hysteretic behaviour of unsheathed X-braced frames is presented.
Kim et al. [75]	1. The use of three channels for the columns at the exterior edges of the frame helps achieve very good performance of the wall even after local buckling. 2. During regions of the earthquake response where the braces give no strength or stiffness, these columns provide energy dissipation.
Abu-Hamd et al. [81]	For walls with aspect ratios of 1:1 and 1:2, the R factor can be enhanced by utilising weaker straps and stronger connectors, chord studs, and tracks.
Zeynalian and Ronagh [82]	1. Knee bracing has a high maximum drift, while its strength is not as high as X-strap bracing. 2. Restricting the use of knee bracing systems to low seismic zones. 3. The use of four interior corners to improve the panel's lateral performance.
Zeynalian and Ronagh [83]	Restricting the use of knee bracing systems to low seismic zones.
Pourabdollah et al. [84]	1. Using gusset plate in braced to stud connections to improve shear strength, energy dissipation, and ductility of K-braced panels. 2. Doubling the chord studs leads to an increase in the shear strength, lateral stiffness, ductility factor, and energy dissipation capabilities.
Tian et al. [85]	The steel-sheathed cold-formed steel trussed shear wall has a significantly higher ultimate strength, unit elastic stiffness, and dissipates more energy.

Table C.2
A summary of research highlights on moment-resisting frames.

Researcher	Research highlights
Lim and Nethercot [3]	The frame with the shorter bolt-group length fails with a load that is roughly 20% lower than the frame with the longer bolt-group length.
Sato and Uang [6]	The response modification coefficient, deflection amplification factor, and system overstrength factor were all presented.
Mojtabaei et al. [19]	Increasing the width-to-thickness ratio of the column results in a significant increase in energy dissipation capacity and the ductility ratio of the proposed system.
Uang et al. [20]	Beams and columns should be designed to maintain their elasticity, while frame energy dissipation should be based on bolt slippage and bearing in moment connections.
Bagheri Sabbagh et al. [86]	1. The CFS curved flange beams increase the nominal plastic moment capacity and sustain this capacity at large rotations. 2. The mobilisation of the bearing action in the connections enables the CFS bolted connections to produce highly stable hysteretic behaviour.
Kirk [87]	Buckling of the web close to the connection zone is the most prevalent failure mode for CFS bolted moment connections.

(*continued on next page*)

Table C.2 (*continued*).

Researcher	Research highlights
Blum and Rasmussen [88]	The efficient design of portal frames depends on the design of connections and modifications to connections.
Blum and Rasmussen [89]	For various bracket thicknesses and apex configurations, the stiffness of the column base connection is investigated.
Lee et al. [90]	The sway stiffness of a light steel frame is affected by joint flexibility and foundation conditions.
Lim et al. [91]	The strength of bolted moment connections between CFS channel members, where the connections are formed through an array of bolts in the web, is dependent on the length of the bolt-group.
McCrum et al. [92]	1. At the section web, the bi-moment stress component accounted for 41% of the total longitudinal stresses. 2. The normal tolerance bolt holes connections performed better under cyclic loading in comparison to the perfect-fit tolerance bolt holes, with 5.4% larger ductility and 22.3% increased energy dissipation.
Lim and Nethercot [94]	To assist engineers in analysing and designing cold-formed steel portal frames, a simple linear beam idealisation of a cold-formed steel portal frame is given.
Rinchen and Rasmussen [93]	1. The failure modes of eaves connections are dominated by bending of eaves brackets and collapse triggered by screw fracture. 2. The apex connections are failed by the inelastic local buckling near the compression flange-web junction.
Zhang et al. [95]	The capacity of locally and distortionally buckled portal frames may be overestimated by the current AS/NZS 4600 and AISI S100 design standards.
Rinchen and Rasmussen [96]	1. Because of the presence of a bimoment at the connections, the ultimate capacity of the tested frames is lower than those obtained from the DSM. 2. The type of fasteners utilised to attach the channel lips to the brackets in the apex and eave connections has a significant impact on the eventual failure deformation.
Dubina et al. [97]	1. The moment resistance of cold-formed members can be reduced by axial forces, which must be considered. 2. A connection with bolts only on the web results in concentrated forces on the connected member's web, causing premature web buckling and a reduction in joint moment capacity.
Wong and Chung [98]	Four different failure modes were identified for bolted moment connections.
Yu et al. [100]	Flexural failure of connected sections is always critical for beam–column sub-frames with large bolt pitches and thick gusset plates in the connections.
ShahMohammadi et al. [102]	1. The governing failure mode was in-plane in both experimental specimens due to the very high torsional resistance of closed box sections. 2. The specimen under cyclic load showed a high level of ductility achieved by forming an inelastic hinge in the mid-point of the left rafter. 3. The nominal rotational stiffness prescribed in NZS 3404 is underestimated for portal frame designs.
McCrum et l. [103]	The hybrid test method was used for the first time to investigate the seismic performance of CFS portal frames under true seismic loading.
Wrzesien et al. [104]	1. The internal frame with roof sheeting resists approximately three times more horizontal load than the bare frame, while skin diaphragm action reduces internal frame deflection by 90% compared to the bare frame. 2. The load transfer between frames is influenced by the joint flexibility of the frame. 3. The size of the brackets is the essential factor in the behaviour of the moment-resisting frames.
Wrzesien et al. [105]	1. The effect of stress–skin action is greater for buildings with the same span and length (i.e., square-shaped), but reduces as more bays are added (i.e., rectangular-shaped). 2. In the cost optimisation procedure, considering the stressed-skin action reduces the cost of the internal frame by around half for square-shaped buildings
Shahini et al. [107]	A circular arrangement of bolts with slotted holes in the gusset plate can delay local buckling failure in the CFS beam and thus improve the cyclic response.
Yin et al. [108]	Two novel configurations of CFS moment-resisting joints improve the rotational capacity and energy dissipation capacities of the joints under cyclic load by postponing the local buckling phenomenon of the connected beams.
Tshuma and Dundu [109]	Two configurations were developed for the connection between the rafters and internal columns.
Teh and Gilbert [110–112]	1. The current shear lag factors cause the code equations to predict a greater net section capacity in a bolted connection if the net section area is reduced. 2. Shear lag factors computed using the AISI S100 and AS/NZS 4600 often exceed unity and have to be ignored in the calculation of the net section tension capacity.
Sato and Uang [106]	Background information was provided for the development of capacity design provisions specified in the AISI's first standard.
Ye et al. [115]	The friction-slip mechanism improves the energy dissipation capacity, ductility, and damping coefficient of the connections by causing a horizontal shift in the hysteretic moment–rotation response.
Bagheri Sabbagh et al. [116]	When designing bolted moment connections, it is recommended to utilise non-uniform rotation by considering bolt slip effects, which requires higher bolt pretension.
Shahini et al. [117]	In CFS beams, the bolting friction mechanism can effectively prevent or delay local buckling.
Bagheri Sabbagh et al. [118]	A new shape of CFS beam with a curved flange is proposed to provide ductility and a beam–column connection through plates.
Bagheri Sabbagh et al. [119]	In the connection region, a minimum of two pairs of vertical stiffeners are required to delay web and flange buckling and produce relatively high moment strength and ductility.
Ye et al. [120]	The use of curved and folded flange channels postpones the local buckling of the flange by creating in-plane stiffness through arching action and shifting the buckling failure to the web.

(*continued on next page*)

Table C.2 (*continued*).

Researcher	Research highlights
Papargyriou et al. [121]	To engage the flanges in the connection behaviour, two innovative CFS beam-to-column connection configurations were developed for seismic applications.
Pouladi et al. [122]	In practice, it is predicted that the screws prevent joint slip during frame erection, however, they control the stiffness of the eaves joints since the bolts did not engage in the first screws' failure.
Lim and Nethercot [123]	The frames proposed based on the simple beam idealisation accounting for the semi-rigidity of the joints provide competitive alternatives to conventional rigid jointed hot-rolled steel connections.
Lim and Nethercot [124]	A method has been proposed to determine the initial rotational stiffness of a shear-type bolted moment-connection.
Chen et al. [125]	Design equations have been developed to predict the strength of moment-resisting apex brackets.
Mojtabaei et al. [126]	When a longer bolt-group length is utilised, the effects of local failure resulting from a complicated stress condition caused by the transfer of both shear and bending moments across the web can be greatly reduced.
Mojtabaei et al. [127]	1. The presence of a shear lag effect could significantly reduce the cross-sectional capacity of the connected member subjected only to compression. 2. The capacity of the connected member exponentially converges to the full cross-sectional capacity with increasing the ratio of the bolt-group length to the eccentricity of the connection as well as decreasing values of the web slenderness ratio.
Lim and Young [128]	The value of bolt-group length does not affect the value of the ultimate moment capacity at elevated temperatures.
Mojtabaei et al. [129]	1. By reducing the width of the beam flanges and increasing the web height, the energy dissipation of the connections increases by up to 15%. 2. The flexural capacity of the connection is generally improved when the optimisation is based on energy dissipation, but the ductility-based optimisation results in a lower flexural capacity. 3. The use of intermediate stiffeners in the beam section can improve the connections' flexural strength and ductility, while the energy dissipation capacity of the connections is reduced slightly. 4. The optimisation of the CFS bolted moment connections under cyclic load leads to the same optimal sections achieved under monotonic load for both energy dissipation and ductility.
Mojtabaei et al. [130]	The best CFS beam sections are generated using the Big Bang-Big Crunch (BB-BC) algorithm, and their flexural capacity and stiffness can be enhanced by up to 58 percent and 44 percent, respectively, compared to their standard counterparts.
Wrzesien et al. [131]	Under various load combinations and constraints, the optimum joint detail was proposed, where the size of the brackets is the essential parameter of importance.
Phan et al. [132]	Combining element and structural level optimisation for CFS portal frame design
ShahMohammadi et al. [133]	The economic viability of a novel proposed system has been investigated by conducting a cost comparison between portal frames with nested tapered box and fabricated tapered I-section using a Genetic Algorithm.
Munse and Chesson [134]	The tensile behaviour of bolted and riveted members was investigated.
Phan et al. [135]	1. A short bolt-group length may lead to up to a 25% reduction in the flexural strength of the CFS bolted connections. 2. Shape optimisation can significantly increase the flexural strength of the CFS bolted moment connections, with more efficiency for the bolted moment connections with a shorter bolt-group length and larger beam length.

References

[1] Wenying Zhang, Mahsa Mahdavian, Cheng Yu, Different slit configuration in corrugated sheathing of cold-formed steel shear wall, J. Construct. Steel Res. 150 (2018) 430–441, http://dx.doi.org/10.1016/j.jcsr.2018.08.035.

[2] Maryam Hasanali, Seyed Mohammad Mojtabaei, G Charles Clifton, Iman Hajirasouliha, Shahabeddin Torabian, James BP. Lim, Capacity and design of cold-formed steel warping-restrained beam–column elements, J. Construct. Steel Res. 190 (2022) 107139, http://dx.doi.org/10.1016/j.jcsr.2022.107139.

[3] James BP. Lim, David A. Nethercot, Ultimate strength of bolted moment-connections between cold-formed steel members, Thin-Walled Struct. 41 (11) (2003) 1019–1039, http://dx.doi.org/10.1016/S0263-8231(03)00045-4.

[4] E.F Gad, C.F. Duffield, G.L. Hutchinson, D.S. Mansell, G. Stark, Lateral performance of cold-formed steel-framed domestic structures, Eng. Struct. 21 (1) (1999) 83–95, http://dx.doi.org/10.1016/S0141-0296(97)90129-2.

[5] Robert L. Madsen, Thomas A. Castle, Benjamin W. Schafer, Seismic design of cold-formed steel lateral load-resisting systems, NEHRP Seism. Des. Tech. Brief 12 (2016).

[6] Atsushi Sato, Chia-Ming Uang, Seismic performance factors for cold-formed steel special bolted moment frames, J. Struct. Eng. 136 (8) (2010) 961–967, http://dx.doi.org/10.1061/(ASCE)ST.1943-541X.0000191.

[7] Pezhman Sharafi, Mina Mortazavi, Bijan Samali, Hamid Ronagh, Prefabricated hybrid wall panel system for lightweight steel construction in Seismic Prone Regions, 2018.

[8] Wenying Zhang, Xiangzhi Xu, Yang Liu, Cheng Yu, Xuechun Liu, Zhiqiang Xie, High-strength cold-formed steel framed shear wall with steel sheet sheathing, Thin-Walled Struct. 162 (2021) 107584, http://dx.doi.org/10.1016/j.tws.2021.107584.

[9] Wenying Zhang, Mahsa Mahdavian, Yuanqi Li, Cheng Yu, Experiments and simulations of cold-formed steel wall assemblies using corrugated steel sheathing subjected to shear and gravity loads, J. Struct. Eng. 143 (3) (2017) 04016193, http://dx.doi.org/10.1061/(ASCE)ST.1943-541X.0001681.

[10] Wenying Zhang, Mahsa Mahdavian, Yuanqi Li, Cheng Yu, Seismic performance evaluation of cold-formed steel shear walls using corrugated steel sheathing, J. Struct. Eng. 143 (11) (2017) 04017151, http://dx.doi.org/10.1061/(ASCE)ST.1943-541X.0001891.

[11] Wenying Zhang, Cheng Yu, Mahsa Mahdavian, Seismic performance of cold-formed steel shear walls using corrugated sheathing with slits, J. Struct. Eng. 145 (4) (2019) 04019014, http://dx.doi.org/10.1061/(ASCE)ST.1943-541X.0002284.

[12] Cheng Yu, Guowang Yu, Experimental investigation of cold-formed steel framed shear wall using corrugated steel sheathing with circular holes, J. Struct. Eng. 142 (12) (2016) 04016126, http://dx.doi.org/10.1061/(ASCE)ST.1943-541X.0001609.

[13] Dan Dubina, Raffaele Landolfo, Viorel Ungureanu, Design of Cold-Formed Steel Structures.: Eurocode 3: Design of Steel Structures. Part 1-3, Design of Cold-Formed Steel Structures, Eccs, 2012.

[14] AS/NZS 4600, Cold-Formed Steel Structures, (Australian Standard/New Zealand Standard), Sydney/Wellington, 2018.

[15] Ioannis Papargyriou, Iman Hajirasouliha, Jurgen Becque, Kypros Pilakoutas, Performance-based assessment of CFS strap-braced stud walls under seismic loading, J. Construct. Steel Res. 183 (2021) 106731, http://dx.doi.org/10.1016/j.jcsr.2021.106731.

[16] Noritsugu Yanagi, Cheng Yu, Effective strip method for the design of cold-formed steel framed shear wall with steel sheet sheathing, J. Struct. Eng. 140 (4) (2014) 04013101, http://dx.doi.org/10.1061/(ASCE)ST.1943-541X.0000870.

[17] AISI (American Iron and Steel Institute), North American Standard for Cold-Formed Steel Framing-Floor and Roof System Design (AISI S210-07), AISI, Washington, DC, 2012.

[18] AISI (American Iron and Steel Institute), North American Standard for Seismic Design of Cold-Formed Steel Structural Systems (AISI S400-15), AISI, Washington, DC, 2015.

[19] Seyed Mohammad Mojtabaei, Mohammad Zaman Kabir, Iman Hajirasouliha, Mina Kargar, Analytical and experimental study on the seismic performance

of cold-formed steel frames, J. Construct. Steel Res. 143 (2018) 18–31, http://dx.doi.org/10.1016/j.jcsr.2017.12.013.
[20] Chia-Ming Uang, Atsushi Sato, Jong-Kook Hong, Ken Wood, Cyclic testing and modeling of cold-formed steel special bolted moment frame connections, J. Struct. Eng. 136 (8) (2010) 953–960, http://dx.doi.org/10.1061/(ASCE)ST.1943-541X.0000190.
[21] Ornella Iuorio, Vincenzo Macillo, Maria Teresa Terracciano, Tatiana Pali, Luigi Fiorino, Raffaele Landolfo, Seismic response of cfs strap-braced stud walls: Experimental investigation, Thin-Walled Struct. 85 (2014) 466–480, http://dx.doi.org/10.1016/j.tws.2014.09.008.
[22] Pezhman Sharafi, Mina Mortazavi, Nima Usefi, Kamyar Kildashti, Hamid Ronagh, Bijan Samali, Lateral force resisting systems in lightweight steel frames: Recent research advances, Thin-Walled Struct. 130 (2018) 231–253, http://dx.doi.org/10.1016/j.tws.2018.04.019.
[23] A Mirzaei, R.H Sangree, K. Velchev, G. Comeau, N. Balh, C.A. Rogers, B.W. Schafer, Seismic capacity-based design of narrow strap-braced cold-formed steel walls, J. Construct. Steel Res. 115 (2015) 81–91, http://dx.doi.org/10.1016/j.jcsr.2015.08.023.
[24] Vincenzo Macillo, Ornella Iuorio, Maria Teresa Terracciano, Luigi Fiorino, Raffaele Landolfo, Seismic response of Cfs strap-braced stud walls: Theoretical study, Thin-Walled Struct. 85 (2014) 301–312, http://dx.doi.org/10.1016/j.tws.2014.09.006.
[25] K Velchev, G. Comeau, N. Balh, C.A. Rogers, Evaluation of the AISI S213 seismic design procedures through testing of strap braced cold-formed steel walls, Thin-Walled Struct. 48 (10–11) (2010) 846–856, http://dx.doi.org/10.1016/j.tws.2010.01.003.
[26] Y.S Tian, Jian Wang, T.J. Lu, Racking strength and stiffness of cold-formed steel wall frames, J. Construct. Steel Res. 60 (7) (2004) 1069–1093, http://dx.doi.org/10.1016/j.jcsr.2003.10.002.
[27] S.A Adham, V. Avanessian, G.C. Hart, R.W. Anderson, J. Elmlinger, J. Gregory, Shear wall resistance of light gage steel stud wall systems, Earthq. Spectra 6 (1) (1990) 1–14, http://dx.doi.org/10.1193/1.1585555.
[28] Reynaud Serrette, Kehinde Ogunfunmi, Shear resistance of gypsum-sheathed light-gauge steel stud walls, J. Struct. Eng. 122 (4) (1996) 383–389, http://dx.doi.org/10.1061/(ASCE)0733-9445(1996)122:4(383).
[29] Mehran Zeynalian, Adelaide Shelley, Hamid R. Ronagh, Shahab Hatami, Experimental investigation into the capacity of cold-formed screwed steel strap bracing connections, Adv. Steel Constr. 14 (4) (2018) 562–588, http://dx.doi.org/10.18057/IJASC.2018.14.4.3.
[30] R Tremblay, M-H. Archambault, A. Filiatrault, Seismic response of concentrically braced steel frames made with rectangular hollow bracing members, J. Struct. Eng. 129 (12) (2003) 1626–1636, http://dx.doi.org/10.1061/(ASCE)0733-9445(2003)129:12(1626).
[31] Shahrzad Kasaeian, Nima Usefi, Hamid Ronagh, Saeed Dareshiry, Seismic performance of CFS strap-braced walls using capacity-based design approach, J. Construct. Steel Res. 174 (2020) 106317, http://dx.doi.org/10.1016/j.jcsr.2020.106317.
[32] Reynaud Serrette, Jose Encalada, Georgi Hall, Brandon Matchen, Hoang Nguygen, Alexander Williams, Additional Shear Wall Values for Light Weight Steel Framing, (FinalReport), Santa Clara University, Santa Clara, CA, 2007.
[33] Miquel Casafont, Alfredo Arnedo, Francesc Roure, Antonio Rodríguez-Ferran, Experimental testing of joints for seismic design of lightweight structures, Part 3: Gussets, corner joints, x-braced frames, Thin-Walled Struct. 45 (7–8) (2007) 637–659, http://dx.doi.org/10.1016/j.tws.2007.05.008.
[34] Giles Comeau, Inelastic performance of welded CFS strap braced walls, 2008.
[35] Luigi Fiorino, Maria Teresa Terracciano, Raffaele Landolfo, Experimental investigation of seismic behaviour of low dissipative CFS strap-braced stud walls, J. Construct. Steel Res. 127 (2016) 92–107, http://dx.doi.org/10.1016/j.jcsr.2016.07.027.
[36] Kostadin Velchev, Colin A. Rogers, Inelastic performance of screw connected CFS strap braced walls, 2008.
[37] AISI (American Iron and Steel Institute), North American Standard for Cold-Formed Steel Framing- Lateral Design 2007 Edition with Supplement No. 1. AISI S213-07, AISI, Washington, DC, 2012.
[38] M Al-Kharat, C.A. Rogers, Inelastic performance of cold-formed steel strap braced walls, J. Construct. Steel Res. 63 (4) (2007) 460–474, http://dx.doi.org/10.1016/j.jcsr.2006.06.040.
[39] Hassan Moghimi, Hamid R. Ronagh, Performance of light-gauge cold-formed steel strap-braced stud walls subjected to cyclic loading, Eng. Struct. 31 (1) (2009) 69–83, http://dx.doi.org/10.1016/j.engstruct.2008.07.016.
[40] Mustafa Al-Kharat, C.A. Rogers, Testing of Light Gauge Steel Strap Braced Walls, Department of Civil Engineering and Applied Mechanics, McGill University, 2005.
[41] Mustafa Al-Kharat, C.A. Rogers, Inelastic performance of screw-connected cold-formed steel strap-braced walls, Can. J. Civil Eng. 35 (1) (2008) 11–26, http://dx.doi.org/10.1139/L07-081.
[42] Mustafa Al-Kharat, C.A. Rogers, Inelastic Performance of Screw Connected Light Gauge Steel Strap Braced Walls, Department of Civil Engineering and Applied Mechanics, McGill University, 2006.
[43] Miquel Casafont, Alfredo Arnedo, Francesc Roure, Antonio Rodríguez-Ferran, Experimental testing of joints for seismic design of lightweight structures. Part 1. Screwed joints in straps, Thin-Walled Struct. 44 (2) (2006) 197–210, http://dx.doi.org/10.1016/j.tws.2006.01.002.
[44] Mique Casafont, Alfredo Arnedo, Francesc Roure, Antonio Rodríguez-Ferran, Experimental testing of joints for seismic design of lightweight structures. Part 2: Bolted joints in straps, Thin-Walled Struct. 44 (6) (2006) 677–691, http://dx.doi.org/10.1016/j.tws.2006.04.006.
[45] EN 1993-1-3, Eurocode 3: Design of Steel Structures-Part 1-3: General Rules: Supplementary Rules for Cold-Formed Members and Sheeting, European Committee for Standardization, Brussels, 2006.
[46] Hassan Moghimi, Hamid R. Ronagh, Better connection details for strap-braced CFS stud walls in seismic regions, Thin-Walled Struct. 47 (2) (2009) 122–135, http://dx.doi.org/10.1016/j.tws.2008.07.003.
[47] M.R. Davani, S. Hatami, A. Zare, Performance-based evaluation of strap-braced cold-formed steel frames using incremental dynamic analysis, Steel Compos. Struct. Int. J. 21 (6) (2016) 1369–1388, http://dx.doi.org/10.12989/scs.2016.21.6.1369.
[48] Maria Teresa Terracciano, Bianca Bucciero, Tatiana Pali, Vincenzo Macillo, Luigi Fiorino, Raffaele Landolfo, Shake table tests of structures with CFS strap-braced stud walls, in: Key Engineering Materials, Vol. 763, Trans Tech Publications Ltd, 2018, pp. 432–439, http://dx.doi.org/10.4028/www.scientific.net/KEM.763.432.
[49] Luigi Fiorino, Bianca Bucciero, Raffaele Landolfo, Shake table tests of three storey cold-formed steel structures with strap-braced walls, Bull. Earthq. Eng. 17 (7) (2019) 4217–4245, http://dx.doi.org/10.1007/s10518-019-00642-z.
[50] Raffaele Landolfo, Alessia Campiche, Ornella Iuorio, Luigi Fiorino, Seismic performance evaluation of CFS strap-braced buildings through experimental tests, in: Structures, Vol. 33, Elsevier, 2021, pp. 3040–3054, http://dx.doi.org/10.1016/j.istruc.2021.05.098.
[51] L.A Fülöp, Dan Dubina, Performance of wall-stud cold-formed shear panels under monotonic and cyclic loading: Part I: Experimental research, Thin-Walled Struct. 42 (2) (2004) 321–338, http://dx.doi.org/10.1016/S0263-8231(03)00063-6.
[52] Wanqian Wang, Jingfeng Wang, T.Y Yang, Lei Guo, Huihui Song, Experimental testing and analytical modeling of CFS shear walls filled with LPM, in: Structures, Vol. 27, Elsevier, 2020, pp. 917–933, http://dx.doi.org/10.1016/j.istruc.2020.06.016.
[53] Bin Liu, Ji-Ping Hao, Wei-Hui Zhong, Hao Wang, Performance of cold-formed-steel-framed shear walls sprayed with lightweight mortar under reversed cyclic loading, Thin-Walled Struct. 98 (2016) 312–331, http://dx.doi.org/10.1016/j.tws.2015.09.024.
[54] Jeffrey W. Berman, Oguz C. Celik, Michel Bruneau, Comparing hysteretic behavior of light-gauge steel plate shear walls and braced frames, Eng. Struct. 27 (3) (2005) 475–485, http://dx.doi.org/10.1016/j.engstruct.2004.11.007.
[55] Mehran Zeynalian, Hamid R. Ronagh, A numerical study on seismic performance of strap-braced cold-formed steel shear walls, Thin-Walled Struct. 60 (2012) 229–238, http://dx.doi.org/10.1016/j.tws.2012.05.012.
[56] Mohsen Gerami, Mohsen Lotfi, Roya Nejat, Inelastic behavior of cold-formed braced walls under monotonic and cyclic loading, Int. J. Adv. Struct. Eng. (IJASE) 7 (2) (2015) 181–209, http://dx.doi.org/10.1007/s40091-015-0091-8.
[57] Ioannis Papargyriou, Iman Hajirasouliha, More efficient design of CFS strap-braced frames under vertical and seismic loading, J. Construct. Steel Res. 185 (2021) 106886, http://dx.doi.org/10.1016/j.jcsr.2021.106886.
[58] Shuna Ni, Xia Yan, Matthew S. Hoehler, Thomas Gernay, Numerical modeling of the post-fire performance of strap-braced cold-formed steel shear walls, Thin-Walled Struct. 171 (2022) 108733, http://dx.doi.org/10.1016/j.tws.2021.108733.
[59] Laura N. Lowes, Nilanjan Mitra, Arash Altoontash, A beam–column joint model for simulating the earthquake response of reinforced concrete frames, 2003.
[60] Luigi Fiorino, Sarmad Shakeel, Vincenzo Macillo, Raffaele Landolfo, Behaviour factor (q) evaluation the CFS braced structures according to FEMA P695, J. Construct. Steel Res. 138 (2017) 324–339, http://dx.doi.org/10.1016/j.jcsr.2017.07.014.
[61] CEN, EN 1998-1-1. Eurocode 8: Design of Structures for Earthquake Resistance-Part 1-1: General Rules, Seismic Actions and Rules for Buildings, European Committee for Standardization, Brussels, 2005.
[62] Alessia Campiche, Numerical modelling of CFS three-story strap-braced building under shaking-table excitations, Materials 14 (1) (2021) 118, http://dx.doi.org/10.3390/ma14010118.
[63] V. Macillo, S. Shakeel, R. Landolfo, Development and calibration of a hysteretic model for CFS strap braced stud walls, Adv. Steel Constr. 14 (3) (2018) 337–360, http://dx.doi.org/10.18057/IJASC.2018.14.3.2.
[64] G. Comeau, K.R.C.A Velchev, C.A. Rogers, Development of seismic force modification factors for cold-formed steel strap braced walls, Can. J. Civil Eng. 37 (2) (2010) 236–249, http://dx.doi.org/10.1139/L09-153.
[65] Athol J. Carr, User Manual for the 3-Dimensional Version Ruaumoko3D, University of Canterbury, Department of Civil Engineering, Computer Program Library, 2012.

[66] AISI (American Iron and Steel Institute), North American Standard for Cold-Formed Steel Framing- Lateral Design 2007 Edition with Supplement No. 1. AISI S213-07/S1-09, AISI, Washington, DC, 2009.
[67] Natividad Pastor, Antonio Rodríguez-Ferran, Hysteretic modelling of x-braced shear walls, Thin-Walled Struct. 43 (10) (2005) 1567–1588, http://dx.doi.org/10.1016/j.tws.2005.06.010.
[68] ASCE 41, Seismic Evaluation and Retrofit of Existing Buildings, American Society of Civil Engineers, 2014.
[69] Applied Technology Council, and Structural Engineers Association of California, Tentative Provisions for the Development of Seismic Regulations for Buildings: A Cooperative Effort with the Design Professions, Building Code Interests, and the Research Community. Vol. 3 (6), Department of Commerce, National Bureau of Standards, 1978.
[70] FEMA P-1050 Council, Building Seismic Safety, NEHRP recommended seismic provisions for new buildings and other structures: Part I (provisions) and part II (commentary), 2015.
[71] UBC, Uniform Building Code, Uniform building code, in: Int. Conf. Building Officials, 1997.
[72] ASCE 7–10, Minimim Design Loads for Buildings and Other Structures, American Society of Civil Engineers, Reston, Virginia, 2010.
[73] National Building Code of Canada, National Research Council of Canada (NRCC), Ottawa, ON, Canada, 2005.
[74] CEN, EN 1998-1. Eurocode 8: Design of Structures for Earthquake Resistance-Part 1: General Rules, Seismic Actions and Rules for Buildings, European Committee for Standardization, Brussels, 2004.
[75] Tae-Wan Kim, James Wilcoski, Douglas A. Foutch, Moon Sung Lee, Shaketable tests of a cold-formed steel shear panel, Eng. Struct. 28 (10) (2006) 1462–1470, http://dx.doi.org/10.1016/j.engstruct.2006.01.014.
[76] TI 809-07, Design of cold-formed loadbearing steel systems and masonry veneer/steel stud walls, 1998.
[77] Luigi Fiorino, Ornella Iuorio, Vincenzo Macillo, Maria Teresa Terracciano, Tatiana Pali, Raffaele Landolfo, Seismic design method for CFS diagonal strap-braced stud walls: experimental validation, J. Struct. Eng. 142 (3) (2016) 04015154.
[78] Canadian Standards Association, CSA-S136: North American Specification for the Design of Cold-Formed Steel Structural Members, Canadian Standards Association, Mississauga, ON, 2001.
[79] ASCE 7-05, Minimum Design Loads for Buildings and Other Structures, American Society of Civil Engineers, 2005, http://dx.doi.org/10.1061/(ASCE)ST.1943-541X.0001408.
[80] FEMA P-695, Qualifications of Building Seismic Performance Factors, Washington, DC, USA, 2009.
[81] Metwally Abu-Hamd, Maheeb Abdel-Ghaffar, Basel El-Samman, Computational study of cold-formed-steel X-Braced shear walls, Adv. Civ. Eng. 2018 (2018) http://dx.doi.org/10.1155/2018/9784360.
[82] Mehran Zeynalian, Hamid R. Ronagh, An experimental investigation on the lateral behavior of knee-braced cold-formed steel shear walls, Thin-Walled Struct. 51 (2012) 64–75, http://dx.doi.org/10.1016/j.tws.2011.11.008.
[83] M. Zeynalian, H.R. Ronagh, S. Hatami, Seismic characteristics of K-braced cold-formed steel shear walls, J. Constr. Steel Res. 77 (2012) 23–31, http://dx.doi.org/10.1016/j.jcsr.2012.04.009.
[84] Omid Pourabdollah, Farhang Farahbod, Fayaz R. Rofooei, The seismic performance of K-braced cold-formed steel shear panels with improved connections, J. Construct. Steel Res. 135 (2017) 56–68, http://dx.doi.org/10.1016/j.jcsr.2017.04.008.
[85] Hui-Wen Tian, Yuan-Qi Li, Cheng Yu, Testing of steel sheathed cold-formed steel trussed shear walls, Thin-Walled Struct. 94 (2015) 280–292.
[86] Sabbagh Bagheri, . Alireza, Mihail Petkovski, Kypros Pilakoutas, Rasoul Mirghaderi, Experimental work on cold-formed steel elements for earthquake resilient moment frame buildings, Eng. Struct. 42 (2012) 371–386, http://dx.doi.org/10.1016/j.engstruct.2012.04.025.
[87] Philip Kirk, Design of a cold formed section portal frame building system, in: Proc. 8th Int. Speciality Conf. on Cold-Formed Steel Structures, Vol. 259, Univ. of Missouri-Rolla, St. Louis, MO, 1986.
[88] H.B. Blum, K.J.R. Rasmussen, Experimental investigation of long-span cold-formed steel double channel portal frames, J. Construct. Steel Res. 155 (2019) 316–330, http://dx.doi.org/10.1016/j.jcsr.2018.11.020.
[89] H.B Blum, K.J.R. Rasmussen, Experimental and numerical study of connection effects in long-span cold-formed steel double channel portal frames, J. Construct. Steel Res. 155 (2019) 480–491, http://dx.doi.org/10.1016/j.jcsr.2018.11.013.
[90] Yeong Huei Lee, Cher Siang Tan, Shahrin Mohammad, In-plane sway behaviour of slender cold-formed steel bolted frames, Thin-Walled Struct. 114 (2017) 11–21, http://dx.doi.org/10.1016/j.tws.2017.01.024.
[91] James BP. Lim, Gregory J. Hancock, G Charles Clifton, Cao Hung Pham, Raj Das, DSM for ultimate strength of bolted moment-connections between cold-formed steel channel members, J. Construct. Steel Res. 117 (2016) 196–203, http://dx.doi.org/10.1016/j.jcsr.2015.10.005.
[92] Daniel P. McCrum, Jordan Simon, Michael Grimes, Brian M. Broderick, James BP Lim, Andrzej M. Wrzesien, Experimental cyclic performance of cold-formed steel bolted moment resisting frames, Eng. Struct. 181 (2019) 1–14, http://dx.doi.org/10.1016/j.engstruct.2018.11.063.
[93] Rinchen Rinchen, Kim JR. Rasmussen, Behaviour and modelling of connections in cold-formed steel single C-section portal frames, Thin-Walled Struct. 143 (2019) 106233, http://dx.doi.org/10.1016/j.tws.2019.106233.
[94] James BP. Lim, David A. Nethercot, Finite element idealization of a cold-formed steel portal frame, J. Struct. Eng. 130 (1) (2004) 78–94, http://dx.doi.org/10.1061/(ASCE)0733-9445(2004)130:1(78).
[95] Zhang Xi, Kim JR Rasmussen, Hao Zhang, Experimental investigation of locally and distortionally buckled portal frames, J. Construct. Steel Res. 122 (2016) 571–583, http://dx.doi.org/10.1016/j.jcsr.2016.04.017.
[96] Rinchen Rinchen, Kim JR. Rasmussen, Experiments on long-span cold-formed steel single C-section portal frames, J. Struct. Eng. 146 (1) (2020) 04019187, http://dx.doi.org/10.1061/(ASCE)ST.1943-541X.0002487.
[97] D Dubina, A Stratan, Zs. Nagy, Full-scale tests on cold-formed steel pitched-roof portal frames with bolted joints, Adv. Steel Constr. 5 (2) (2009) 175–194.
[98] M.F Wong, Kwok Fai Chung, Structural behaviour of bolted moment connections in cold-formed steel beam–column sub-frames, J. Construct. Steel Res. 58 (2) (2002) 253–274, http://dx.doi.org/10.1016/S0143-974X(01)00044-X.
[99] AISI (American Iron and Steel Institute), Standard for Seismic Design of Cold-Formed Steel Structural Systems-Special Bolted Moment Frames, AISI S 110-07, Washington, DC, 2007.
[100] W.K Yu, Kwok Fai Chung, M.F. Wong, Analysis of bolted moment connections in cold-formed steel beam–column sub-frames, J. Construct. Steel Res. 61 (9) (2005) 1332–1352, http://dx.doi.org/10.1016/j.jcsr.2005.03.001.
[101] AISI (American Iron and Steel Institute), North American Specification for the Design of Cold-Formed Steel Structural Members (AISI S100-16), AISI, Washington, DC, 2016.
[102] A. Shahmohammadi, J.B. Lim, C. Clifton, M. Hajsadeghi, Full-scale experimental tests on portal frames comprising novel cold-formed tapered box sections, J. Struct. Eng. 148 (9) (2022) 04022133.
[103] Daniel Patrick McCrum, Jordan Simon, Michael Grimes, Brian Michael Broderick, Andrzej Wrzesien, James Boon Piang Lim, Hybrid seismic testing of cold-formed steel moment-resisting frames, Proc. Inst. Civ. Eng.-Struct. Build. 173 (2) (2020) 88–98, http://dx.doi.org/10.1680/jstbu.18.00017.
[104] A.M Wrzesien, James BP. Lim, Yixiang Xu, Iain A. MacLeod, R.M. Lawson, Effect of stressed skin action on the behaviour of cold-formed steel portal frames, Eng. Struct. 105 (2015) 123–136, http://dx.doi.org/10.1016/j.engstruct.2015.09.026.
[105] Andrzej M. Wrzesien, Duoc T. Phan, James BP. Lim, Hieng-Ho Lau, Iman Hajirasouliha, Cher Siang Tan, Effect of stressed-skin action on optimal design of cold-formed steel square and rectangular-shaped portal frame buildings, Int. J. Steel Struct. 16 (2) (2016) 299–307, http://dx.doi.org/10.1007/s13296-016-6004-2.
[106] Atsushi Sato, Chia-Ming Uang, Seismic design procedure development for cold-formed steel–special bolted moment frames, J. Construct. Steel Res. 65 (4) (2009) 860–868, http://dx.doi.org/10.1016/j.jcsr.2008.03.016.
[107] Marzie Shahini, Alireza Bagheri Sabbagh, Cold-formed steel bolted moment-resisting connections with friction-slip mechanism for seismic areas, 2018.
[108] Lingfeng Yin, Yu Niu, Guan Quan, Han Gao, Jun Ye, Development of new types of bolted joints for cold-formed steel moment frame buildings, J. Build. Eng. (2022) 104171, http://dx.doi.org/10.1016/j.jobe.2022.104171.
[109] B Tshuma, M. Dundu, Internal eaves connections of double-bay cold-formed steel portal frames, Thin-Walled Struct. 119 (2017) 760–769, http://dx.doi.org/10.1016/j.tws.2017.07.023.
[110] Lip H. Teh, Benoit P. Gilbert, Net section tension capacity of bolted connections in cold-reduced steel sheets, J. Struct. Eng. 138 (3) (2012) 337–344, http://dx.doi.org/10.1061/(ASCE)ST.1943-541X.0000477.
[111] Lip H. Teh, Benoit P. Gilbert, Net section tension capacity of cold-reduced sheet steel angle braces bolted at one leg, J. Struct. Eng. 139 (3) (2013a) 328–337, http://dx.doi.org/10.1061/(ASCE)ST.1943-541X.0000675.
[112] Lip H. Teh, Benoit P. Gilbert, Net section tension capacity of cold-reduced sheet steel channel braces bolted at the web, J. Struct. Eng. 139 (5) (2013) 740–747, http://dx.doi.org/10.1061/(ASCE)ST.1943-541X.0000650.
[113] AISI (American Iron and Steel Institute), North American Specification for the Design of Cold-Formed Steel Structural Members, AISI, Washington, DC, 2007.
[114] AS/NZS 4600, Cold-Formed Steel Structures, (Australian Standard/New Zealand Standard), Sydney, 2005.
[115] Jun Ye, Seyed Mohammad Mojtabaei, Iman Hajirasouliha, Seismic performance of cold-formed steel bolted moment connections with bolting friction-slip mechanism, J. Construct. Steel Res. 156 (2019) 122–136, http://dx.doi.org/10.1016/j.jcsr.2019.01.013.
[116] Sabbagh Bagheri, . Alireza, Mihail Petkovski, Kypros Pilakoutas, Rasoul Mirghaderi, Cyclic behaviour of bolted cold-formed steel moment connections: FE modelling including slip, J. Construct. Steel Res. 80 (2013) 100–108, http://dx.doi.org/10.1016/j.jcsr.2012.09.010.

[117] Marzie Shahini, Alireza Bagheri Sabbagh, Paul Davidson, Rasoul Mirghaderi, Development of cold-formed steel moment-resisting connections with bolting friction-slip mechanism for seismic applications, Thin-Walled Struct. 141 (2019) 217–231, http://dx.doi.org/10.1016/j.tws.2019.04.011.

[118] Sabbagh Bagheri, . Alireza, Mihail Petkovski, Kypros Pilakoutas, Rasoul Mirghaderi, Ductile moment-resisting frames using cold-formed steel sections: An analytical investigation, J. Construct. Steel Res. 67 (4) (2011) 634–646, http://dx.doi.org/10.1016/j.jcsr.2010.11.016.

[119] Sabbagh Bagheri, . Alireza, Mihail Petkovski, Kypros Pilakoutas, Rasoul Mirghaderi, Development of cold-formed steel elements for earthquake resistant moment frame buildings, Thin-Walled Struct. 53 (2012) 99–108, http://dx.doi.org/10.1016/j.tws.2012.01.004.

[120] Jun Ye, Seyed Mohammad libaei, Iman Hajirasouliha, Kypros Pilakoutas, Efficient design of cold-formed steel bolted-moment connections for earthquake resistant frames, Thin-Walled Struct. 150 (2020) http://dx.doi.org/10.1016/j.tws.2018.12.015.

[121] Ioannis Papargyriou, Seyed Mohammad Mojtabaei, Iman Hajirasouliha, Jurgen Becque, Kypros Pilakoutas, Cold-formed steel beam-to-column bolted connections for seismic applications, Thin-Walled Struct. 172 (2022) 108876, http://dx.doi.org/10.1016/j.tws.2021.108876.

[122] Pouya Pouladi, John Ronaldson, G Charles Clifton, Jason M. Ingham, Andrzej M. Wrzesien, James BP. Lim, Finite-element assisted design of eaves joint of cold-formed steel portal frames having single channel-sections, in: Structures, Vol. 20, Elsevier, 2019, pp. 452–464, http://dx.doi.org/10.1016/j.istruc.2019.05.009.

[123] J.B.P Lim, D.A. Nethercot, Design and development of a general cold-formed steel portal framing system, Struct. Eng. 80 (21) (2002) 31–39.

[124] James BP. Lim, D.A. Nethercot, Stiffness prediction for bolted moment-connections between cold-formed steel members, J. Construct. Steel Res. 60 (1) (2004) 85–107, http://dx.doi.org/10.1016/S0143-974X(03)00105-6.

[125] Xin Chen, H.B Blum, Krishanu Roy, Pouya Pouladi, Asraf Uzzaman, James BP. Lim, Cold-formed steel portal frame moment-resisting joints: Behaviour, capacity and design, J. Construct. Steel Res. 183 (2021) 106718, http://dx.doi.org/10.1016/j.jcsr.2021.106718.

[126] Seyed Mohammad Mojtabaei, Jurgen Becque, Iman Hajirasouliha, Local buckling in cold-formed steel moment-resisting bolted connections: behavior, capacity, and design, J. Struct. Eng. 146 (9) (2020) 04020167, http://dx.doi.org/10.1061/(ASCE)ST.1943-541X.0002730.

[127] Seyed Mohammad Mojtabaei, Jurgen Becque, Iman Hajirasouliha, Behavior and design of cold-formed steel bolted connections subjected to combined actions, J. Struct. Eng. 147 (4) (2021) 04021013, http://dx.doi.org/10.1061/(ASCE)ST.1943-541X.0002966.

[128] James BP. Lim, Ben Young, Effects of elevated temperatures on bolted moment-connections between cold-formed steel members, Eng. Struct. 29 (10) (2007) 2419–2427, http://dx.doi.org/10.1016/j.engstruct.2006.11.027.

[129] Seyed Mohammad Mojtabaei, Iman Hajirasouliha, Jun Ye, Optimisation of cold-formed steel beams for best seismic performance in bolted moment connections, J. Construct. Steel Res. 181 (2021) 106621, http://dx.doi.org/10.1016/j.jcsr.2021.106621.

[130] Seyed Mohammad Mojtabaei, Jun Ye, Iman Hajirasouliha, Development of optimum cold-formed steel beams for serviceability and ultimate limit states using Big Bang-Big crunch optimisation, Eng. Struct. 195 (2019) 172–181, http://dx.doi.org/10.1016/j.engstruct.2019.05.089.

[131] A Wrzesien, James BP Lim, D.A. Nethercot, Optimum joint detail for a general cold-formed steel portal frame, Adv. Struct. Eng. 15 (9) (2012) 1623–1639, http://dx.doi.org/10.1260/1369-4332.15.9.1623.

[132] Duoc T. Phan, Seyed Mohammad Mojtabaei, Iman Hajirasouliha, Jun Ye, James BP. Lim, Coupled element and structural level optimisation framework for cold-formed steel frames, J. Construct. Steel Res. 168 (2020) 105867, http://dx.doi.org/10.1016/j.jcsr.2019.105867.

[133] Amir Shahmohammadi, James BP Lim, George Charles Clifton, Portal Frames with a Novel Cold-Formed Tapered Box-Section. in Key Engineering Materials, Vol. 763, Trans Tech Publications Ltd, 2018, pp. 301–309.

[134] William H. Munse, Eugene Chesson Jr., Riveted and bolted joints: net section design, J. Struct. Div. 89 (1) (1963) 107–126, http://dx.doi.org/10.1061/JSDEAG.0000869.

[135] Duoc T. Phan, Seyed Mohammad Mojtabaei, Iman Hajirasouliha, T.L. Lau, James BP. Lim, Design and optimization of cold-formed steel sections in bolted moment connections considering bimoment, J. Struct. Eng. 146 (8) (2020) 04020153, http://dx.doi.org/10.1061/(ASCE)ST.1943-541X.0002715.

[136] CEN Eurocode 3: Design of Steel Structures-Part 1-8: Design of Joints, European Committee for Standardization, Brussels, 2005.